

Response to Reviewer #2:

Chen et al. attempted to elucidate how PM pollution in eastern China will response to future GHG warming, using a large ensemble of CESM simulations. The authors reported that GHG-induced climate change will increase PM pollution days, especially the most severe polluted days ($PM_{2.5} > 75 \mu g m^{-3}$), at the end of 21th century and they argued that reduced tropospheric winds and light precipitation days can be the reasons. Their results are interesting and could deepen our understanding of the impacts of climate change on air quality. The topic is suitable for ACP readers, and this paper is well structured. However, I have some concerns about the linkage between pollution increase and changes in meteorology. The authors need to address the following comments before it can be published.

Reply: Greatly thanks for your valuable comments and suggestion, which have been fully considered and corrected in the current manuscript.

General Comments:

- The authors found an increase of 68% in the most severe pollution days, with only an increase of 3% for light pollution days, but they attributed such increase to the mean change of future GHG-induced climate change. In statistics, I think the increase in most severe pollution days represents the extreme cases, whose linkage to mean climate change needs to be further explored, or at least discussed.

Reply: Thanks for this comment. Yes, the severe pollution events are the extreme cases that largely associated with extreme anomalies of the meteorological conditions. However, it is a great challenge to discuss the changes of the associated meteorological factors for each extreme case, due to the low capability of current model simulation in extremes. In this study, we mainly focus on the impact of mean climate changes on the air pollutions. As we all know, if the mean climate state moves to a level that not favorable for the air pollutant dissipation, the change of the mean meteorological condition would increase the occurring probability of the extreme pollution days. This is the main view we hope to show in this study.

According to the suggestions from you and another reviewer, we have re-organized some expressions referring to the changes of pollution days. More information can be found in the following or in the manuscript.

→ 【Line 239-257】

The increase in $\text{PM}_{2.5}$ surface concentration throughout the 21st century substantially leads to the significant increase of the light anthropogenic $\text{PM}_{2.5}$ pollution days ($\text{PM}_{2.5} > 25 \mu\text{g}/\text{m}^3$) across the northwestern part of eastern China (Fig. 3). Due to the decrease of $\text{PM}_{2.5}$ concentration over the southeastern part of eastern China, the light anthropogenic air pollution days can be expected to decrease in this region. Estimation shows that the number of the light air pollution days would be decreased by approximately 10 days at the end of the 21st century with respect to the early period of this century in the region. However, the annual mean light air pollution days is reported to increase averaged over the eastern China at the end of this century despite the aerosol emission is constant throughout the experiment. In contrast to the light air pollution days, the severe anthropogenic air pollution days ($\text{PM}_{2.5} > 75 \mu\text{g}/\text{m}^3$) show a positive response to the GHG-induced warming across eastern China, particularly for the regions around JJJ in which the high $\text{PM}_{2.5}$ concentration was localized (Fig. 3). The severe air pollution days is estimated to increase by more than 2 days at the end of this century when compared to the early period over this region. Considering the underestimation in aerosol concentration by CESM1 model in China, the percentile threshold metric is also applied here to estimate the future changes in light (90th) and severe (99th) air pollution days. Similar results can be obtained (Fig. S8).

- The ACCMIP (Lamarque et al., 2013) also archives similar simulations by several climate models. It would be helpful if the authors can compare their results with ACCMIP models. Just a suggestion.

Reply: Thanks for your recommendation. We have read this paper carefully and found some interesting and valuable information, which has substantially improved

our knowledge. However, we have not added the comparison discussions of the ACCMIP simulations with the CESM1 results, mainly due to the three reasons. First, the analyses in this study are implemented mainly from the global scale, which shows weak comparison with our analyses that just limited in China. Second, the ACCMIP simulations are forced along the RCP8.5 emissions, but the aerosol emissions are fixed at the current level in CESM1 simulations. The comparison may be not much robust due to the different model and different forcing. Third, we have added the comparison discussion between the simulations that forced along the RCP8.5 trajectory and the fixed aerosol emission from CESM1 model.

→ **【Line 210-219】**

For comparison, we also evaluated the future changes of PM_{2.5} concentrations and the associated species along the RCP8.5 forcing trajectory from the large ensemble simulations of CESM1 (Figure not shown). Different from changes of aerosol concentrations under the fixed aerosol simulations, the PM_{2.5} concentrations and the associated species present uniformly decreasing trends across eastern China from the simulations along the RCP8.5 forcing. The decreasing trends in the RCP8.5 simulations are mainly attributed to the prescribed decrease of aerosol forcing in the future in RCP database (Xu and Lin, 2017). The climate change induced by the GHG-warming might exacerbate the air pollution, but the impacts cannot compensate the prescribed decreasing trend of aerosol concentration.

Specific Comments:

-Line 32-34: As indicated above, the authors should take care here.

Reply: Thanks for this suggestion. We have toned down this expression.

→ **【Line 36-38】**

Further research indicates that the increased stagnation days and the decreased light precipitation days are the possible causes of the increase in PM_{2.5} concentration, as well as the anthropogenic air pollution days.

-Line 134-140: The relationship between air stagnation index used here and PM_{2.5} pollution in China may be not well correlated (e.g., Feng et al., 2018).

Reply: The performance of this stagnation index over China has been evaluated by some early studies. They suggested that this air stagnation definition might not be applicable for China to represent the air pollution condition under the seasonal scales (Feng et al., 2018; Wang et al., 2018). However, the annual mean stagnation generally presents good agreement with that of air pollution across China (Huang et al., 2017; 2018). Here, we mainly focus on the future changes of PM_{2.5} pollution as well as the meteorological conditions from the annual mean perspective. This definition is thus suit to the stagnation analysis in this study. More information can be found in the following or in the current manuscript.

Feng, J., Quan, J., Liao, H., Li, Y., and Zhao, X.: An air stagnation index to qualify extreme haze events in northern China, *J. Atmos. Sci.*, doi:10.1175/JAS-D-17-0354.1, 2018.

Huang, Q., Cai, X., Song, Y., and Zhu, T.: Air stagnation in China (1985-2014): Climatological mean features and trends, *Atmos. Chem. Phys.*, 17, 7793-7805, 2017.

Huang, Q., Cai, X., Wang, J., Song, Y., and Zhu, T.: Climatological study of the boundary-layer air stagnation index for China and its relationship with air pollution, *Atmos. Chem. Phys.*, 18, 7573-7593, 2018.

Wang, X., Dickinson, R., Su, L., Zhou, C., and Wang, K.: PM_{2.5} pollution in China and how it has been exacerbated by terrain and meteorological conditions, *Bull. Amer. Meteorol. Soc.*, 99(1), 105-119, 2018.

→ **【Line 146-152】**

Early studies have suggested that this air stagnation definition might not be applicable for China to represent the air pollution condition under the seasonal scales (Feng et al., 2018; Wang et al., 2018). However, the annual mean stagnation generally presents good agreement with that of air pollution across China (Huang et al., 2017; 2018).

The changes in the annual mean states of air stagnations over China at the end of 21st century will thus be discussed in the following.

-Line 148 and Figure 1: Why chose a reference concentration of $75 \mu\text{g m}^{-3}$. The annual PM_{2.5} standard in China is $35 \mu\text{g m}^{-3}$.

Reply: This reference concentration of $75 \mu\text{g m}^{-3}$ is selected in this study according to the guideline value from the World Health Organization (2014). The 24-hour concentration of PM_{2.5} exceeding $75 \mu\text{g m}^{-3}$ is considered as the standard value of Interim target-1 that presented a high possibility of exposing people to serious health hazards. This value is determined basing on published risk coefficients from multi-centre studies and meta-analyses. Some related discussions have been available in the manuscript.

World Health Organization: Air quality guidelines: Global update 2005. World Health Organization Rep., 496 pp., www.euro.who.int/_data/assets/pdf_file/0005/78638/E90038.pdf, 2014.

→ **【Line 160-165】**

According to the statistics, there are approximately 95% sites where the annual mean PM_{2.5} concentration exceeded the WHO recommended 24-hour standard ($25 \mu\text{g/m}^3$) across eastern China, and there are 65 sites centralized by Beijing, where the annual mean PM_{2.5} concentration was larger than $75 \mu\text{g/m}^3$, which would present the possibility of exposing people to serious health hazards (World Health Organization, 2014).

-Line 170-172: The correlation is based on what observational and model data. Should make it clear.

Reply: This spatial correlation is calculated between the site observation and median ensemble of CESM1 simulations.

→ 【Line 182-184】

A strong spatial correlation (0.69) is found for the annual mean PM_{2.5} concentration between the site observation and median ensemble of CESM1 simulations over eastern China (Fig. S1).

-Line 173-175: Same as above, the low bias in model depends on what observational PM_{2.5} you used. As reported in Li et al. (2016), the RCP emissions for year 2005 underestimated anthropogenic emissions of aerosol precursors over China. Thus, the lower PM_{2.5} concentration in model could also partly attribute to underestimated emissions.

Reply: Thanks for this valuable comment. This discussion has been corrected and more information can be found in the following or in the current manuscript.

→ 【Line 186-190】

However, a negative bias is obvious. Early studies (Li et al., 2016; Yang et al., 2017b; c) have documented that this low bias of aerosol concentration simulated by models is much more complicated in China and the causes mainly involve the uncertainties from aerosol emission amount, emission injection height, lack of nitrate, aerosol treatment in model as well as the coarse model resolution.

-Line 182-183: Which region you average the PM_{2.5} concentration for “eastern China”?

Reply: In this study, the region of east to 100 °E is considered as the eastern China, which has been indicated in the manuscript.

→ 【Line 101-103】

In our study region of eastern China (east to 100 °E), there are 1263 sites remaining after the sites with missing values were removed during 2015-2017.

-Line 205: What “SC” shorts for?

Reply: Thanks for this comment. “SC” in the early manuscript is short for “Sichuan Basin”, which has been corrected to “SCB” in the current manuscript. It has been corrected through the manuscript and all figures.

1 **Anthropogenic Fine Particulate Matter Pollution Will Be Exacerbated in Eastern**
2 **China Due to 21st-Century GHG Warming**

3 Huopo Chen^{1,2*}, Huijun Wang^{2,1}, Jianqi Sun^{1,2}, Yangyang Xu³, and Zhicong Yin²

4 ¹ *Nansen-Zhu International Research Centre, Institute of Atmospheric Physics,*
5 *Chinese Academy of Sciences, Beijing, China*

6 ² *Collaborative Innovation Center on Forecast and Evaluation of Meteorological*
7 *Disasters, Nanjing University for Information Science and Technology, Nanjing,*
8 *China*

9 ³ *Department of Atmospheric Sciences, Texas A&M University, College Station Texas,*
10 *USA*

11
12 **Corresponding author:** Huopo Chen (chenhuopo@mail.iap.ac.cn)

13 **Address:** Nansen-Zhu International Research Centre, Institute of Atmospheric
14 Physics, Chinese Academy of Sciences, PO Box 9804, Beijing 100029,
15 China

16 **Email:** chenhuopo@mail.iap.ac.cn

17 **Tel:** (+86)010-82995057

Abstract

China has experienced a substantial increase in severe haze events over the past several decades, which is primarily attributed to the increased pollutant emissions caused by its rapid economic development. The climate changes observed under the warming scenarios, especially those induced by increases in greenhouse gases (GHG), are also conducive to the increase in air pollution. However, how the air pollution changes in response to the GHG warming has not been thoroughly elucidated to date. We investigate this change using the century-long large ensemble simulations with the Community Earth System Model 1 (CESM1) with the fixed anthropogenic emissions at the year 2005. Our results show that although the aerosol emission is assumed to be a constant throughout the experiment, anthropogenic air pollution presents ~~robust~~ positive responses to the GHG-induced warming~~—~~. The anthropogenic PM_{2.5} concentration is estimated to increase averaged over eastern China at the end of this century, but varying from regions, with an increase over northwestern part of eastern China and a decrease over southeastern part. Similar changes can be observed for the light air pollution days. However, the severe air pollution days is reported to increase across eastern China at the end of this century, particularly around the Jing-Jin-Ji region. with an increase of approximately 68% to be observed in the most severe days at the end of the 21st century. Further research indicates that the increased stagnation days and the decreased light precipitation days are the ~~primary-possible~~ causes of the increase in PM_{2.5} concentration, as well as the anthropogenic air pollution days. Estimation shows that the effect of climate change induced by the GHG warming can

41 account for 11%-28% of the changes in anthropogenic air pollution days over eastern
42 China. Therefore, in the future, more stringent regulations on regional air pollution
43 emissions are needed to balance the effect from climate change.

44

1. Introduction

The extraordinarily rapid development of China has caused extremely high aerosol loading and gaseous pollutant emissions that have enveloped most regions across China in the recent decades. The increased pollutant emissions, particularly for the particulate matter finer than 2.5 μm in aerodynamic diameter ($\text{PM}_{2.5}$), generally result in severe haze events and present a major threat to public health (Gao et al., 2017; Tang et al., 2017; Wang, 2018-), crop production (Tie et al., 2016), and regional climates (Cao et al., 2016). For example, the annual averaged $\text{PM}_{2.5}$ in Beijing exceeded 75 $\mu\text{g}/\text{m}^3$ during 2009-2016 (Fig. 1b), which more than three times the recommended 24-hour standard (25 $\mu\text{g}/\text{m}^3$) of the World Health Organization (WHO). This degeneration of the air pollution across China, which is similar to that in Beijing, is primarily caused by the integrated effects of high emissions and poor ventilation (Chen and Wang, 2015; Zhang et al., 2016a). Many efforts are thus underway to reduce emissions that cause severe haze pollutions. However, the question remains of whether climate change will offset or facilitate these efforts.

Recent studies have documented that the exacerbation of air quality over eastern China was partly modulated by meteorological conditions and climate variability that are generally conducive to the severe haze occurrences (Li et al., 2018; Liao and Chang, 2014; Wang and Chen, 2016; Yang et al., 2016; Zhang et al., 2014; Zhang et al., 2016b). Specifically, Wang *et al.* (2015) revealed that the shrinking Arctic sea ice favors less cyclone activity and a more stable atmosphere conducive to haze formation, which can explain approximately 45%-67% of the interannual to

interdecadal variability of winter haze days over eastern China. Besides Arctic sea ice, other decadal variability and changes, including weak East Asian winter monsoon (Jeong et al., 2017; Li et al., 2016; Yin et al., 2015), strong El Niño-Southern oscillation (Gao and Li, 2015; Zhao et al., 2018), high Pacific decadal oscillation (Zhao et al., 2016), and high Arctic oscillation (Cai et al., 2017), may have contributed. In addition, the increasing winter haze days over eastern China may also be linked to the low boundary layer height (Huang et al., 2018; Wang et al., 2018), weakened northerly winds (Yang et al., 2017a), decreased relative humidity (Ding and Liu, 2014), and increased sea surface temperature (Xiao et al., 2015; Yin and Wang, 2016; Yin et al., 2017).

Global warming generally presents an adverse impact on the haze pollution across China. Simulations of the dynamic downscaling by the regional climate model RegCM4 under the RCP4.5 (Representative Concentration Pathway) scenarios have shown that the air environment carrying capacity tends to decrease, and the weak ventilation days tend to increase, in the 21st century across China, suggesting an increase in the haze pollution potential compared to the current state (Han et al., 2017). Furthermore, Cai *et al.* (2017) projected that the days conducive to severe haze pollution in Beijing would increase by 50% at the end of the 21st century (2050-2099) under the RCP8.5 scenarios compared to the historical period.

These qualitative estimations of the haze pollution response to climate changes generally derived from the *potential* changes of the corresponding meteorological conditions indirectly. No studies to date quantitatively assessed the simulated PM

directly. How the fine particulate matter pollution changes in response to the global warming in China has not been thoroughly elucidated to date. This study particularly focuses on the anthropogenic PM_{2.5} loading and its response to the future warming. In this study, the large ensemble simulations from the Community Earth System Model Version 1 (CESM1) throughout the 21st century that are induced by increasing greenhouse gases (GHG) emissions along the trajectory RCP8.5 but retaining the emissions of aerosols and/or their precursors fixed at the year of 2005 level (RCP8.5_FixAerosol2005; Xu and Lamarque, 2018) will be utilized.

2. Data and methods

2.1 PM_{2.5} observational datasets

Surface hourly PM_{2.5} concentration data released since 2013 are taken from the website of the Ministry of Environmental Protection (<http://106.37.208.233:20035>), which covers 1602 sites across China. The duration of available datasets varies across sites because of the gradual development of the monitoring network in recent years. In our study region of eastern China (east to 100 °E), there are 1263 sites remaining after the sites with missing values were removed during 2015-2017. Additionally, surface daily PM_{2.5} concentrations for the Beijing, Shanghai, Guangzhou, and Chengdu cities that had relatively longer monitoring times are also collected from the U.S. Beijing Embassy (<http://www.stateair.net/web/historical/1/1.html>).

2.2 CESM1 model simulations

The CESM1 is an Earth system model involving the atmosphere, land, ocean,

and sea-ice components with a nominal 1° by 1° horizontal resolution (Hurrell et al., 2013). The RCP8.5_FixAerosol2005 simulations are forced by the RCP8.5 scenario, but all emissions of sulfate (SO₄), black carbon (BC) and primary organic matter (POM), and secondary organic aerosols (SOA; or their precursors) and atmospheric oxidants are fixed at the present-day level (2005). These simulations include 16 ensemble members, differing solely in their atmospheric initial conditions with a tiny random temperature difference (order of 10⁻¹⁴ °C; Kay et al., 2015). For comparison, the CESM1 large ensemble consists of 35-member simulations that forced by the RCP8.5 scenario are also employed here. Using ~~this~~-these relatively large ensembles can substantially reduce the contribution of natural variability of the climate system to the result estimation (Xu and Lamarque, 2018).

For the aerosol emission in the RCP scenarios database, just its decadal change is considered rather than the emission at a single year (Lamarque et al., 2011). Here, the years of 2006-2015 are considered as the reference period in the RCP8.5_FixAerosol2005 simulations. The differences of the mean climates from the reference period are largely due to the increase in GHG emissions and are not attributed to the decline in aerosol emissions, as specified in RCP8.5. The changes of anthropogenic PM_{2.5} loadings and anthropogenic air pollution days in our study are thus only a result of the GHG-induced climate change, rather than changes in aerosol emission. Note that just four species of PM_{2.5} components that show a substantial threat to public health are considered here for analysis, including SO₄, BC, POM, and SOA from the CESM1 simulations.

2.3 Definition of the fraction of attributable risk

The influences of the GHG-induced climate changes on the anthropogenic air pollutions in China are investigated using the metric of the fraction of attributable risk (FAR), which has been widely used for attribute analyses of climate extreme changes (Chen and Sun, 2017; Stott et al., 2004). FAR is defined as the $1 - P_0/P_I$, where P_0 is the probability of exceeding a certain threshold during the reference period and P_I is the probability exceeding the same threshold during a given period. FAR thus presents the quantitative estimations of effects of the GHG-induced climate changes on the anthropogenic air pollutions.

2.4 Definition of stagnation days

The changes of the stagnation days that were induced by the increase of GHG emissions are also evaluated in our study to explore the possible impact of climate change on the anthropogenic air pollutions. The day is considered to be stagnant when the daily mean near-surface wind speed is less than 3.2 m/s, the daily mean 500-hPa wind speed is less than 13 m/s, and the daily accumulated precipitation is less than 1 mm (Horton et al., 2012). Early studies have suggested that this air stagnation definition might not be applicable for China to represent the air pollution condition under the seasonal scales (Feng et al., 2018; Wang et al., 2018). However, the annual mean stagnation generally presents good agreement with that of air pollution across China (Huang et al., 2017; 2018). The changes in the annual mean states of air stagnations over China at the end of 21st century will thus be discussed in the following.

3. Results

3.1 Observational changes in PM_{2.5} pollutions

The days of severe haze pollution increased over the past several decades across eastern China, particularly for the episodes of January 2013, December 2015, and December 2016, when several severe haze alerts were reached. High PM_{2.5} loading was centralized over the Jing-Jin-Ji (JJJ) region, Shangdong, and Henan provinces, as well as the Sichuan Basin ([SCB](#), Fig. 1a). The annual mean PM_{2.5} mass concentrations for most sites over these regions exceed 75 $\mu\text{g}/\text{m}^3$. According to the statistics, there are approximately 95% sites where the annual mean PM_{2.5} concentration exceeded the WHO recommended 24-hour standard (25 $\mu\text{g}/\text{m}^3$) across eastern China, and there are 65 sites centralized by Beijing, where the annual mean PM_{2.5} concentration was larger than 75 $\mu\text{g}/\text{m}^3$, which would present the possibility of exposing people to serious health hazards (World Health Organization, 2014).

Regarding the four economic zones of Beijing, Shanghai, Guangzhou, and Chengdu cities over China, serious PM_{2.5} pollution can be expected in recent years, especially for the Beijing and Chengdu regions (Fig. 1). Taking Beijing as an example, the annual mean PM_{2.5} concentration was stably exceeding 100 $\mu\text{g}/\text{m}^3$, and more than a half of the year had experienced severe air pollution ($> 75 \mu\text{g}/\text{m}^3$) before 2013. Since 2013, China's State Council released its Air Pollution Prevention and Control Action Plan, which requires the key regions, including the JJJ, the Yangtze River Delta (YRD), and the Pearl River Delta (PRD) to reduce their atmospheric levels of PM_{2.5} by 25%, 20%, and 15%, respectively, by the end of year 2017 (State Council,

2013). Effort is obvious, and the PM_{2.5} loading and the air pollution days present sharp decreases in recent years. However, the strict emission policies substantially cost the economic development, which cannot meet the current requirement of the rapid development of China. Thus, scientifically quantifying the roles of anthropogenic emissions and climate changes shows great importance for seeking the balance between socioeconomic development and emission reduction.

3.2 Simulated changes in anthropogenic PM_{2.5} pollutions

A strong spatial correlation (0.69) is found for the annual mean PM_{2.5} concentration between the site observation and median ensemble of CESM1 simulations over eastern China (Fig. S1). The high concentrations across eastern China, including the regions centralized by Beijing and Chengdu, are reasonably reproduced. However, a negative bias is obvious, ~~primarily because only four major species are considered in this study from the CESM1 simulations. Early studies (Li et al., 2016; Yang et al., 2017b; c) have documented that this low bias of aerosol concentration simulated by models is much more complicated in China and the causes mainly involve the uncertainties from aerosol emission amount, emission injection height, lack of nitrate, aerosol treatment in model as well as the coarse model resolution.~~

The median ensemble-mean change of the PM_{2.5} surface concentration presents strong regional dependence across China with significantly decreasing trends over the southeastern part of eastern China and significantly increasing trends over the other regions throughout the 21st century (Fig. S2), even though the emissions are constant

throughout the experiment. The regional differences in the total $\text{PM}_{2.5}$ changes are mainly due to SO_4 , which can account for approximately 50% of the total $\text{PM}_{2.5}$ mass (Xu and Lamarque, 2018). The species of BC and POM are reported to significantly increase in the 21st century across eastern China, although the aerosol emissions were fixed at the level in 2005. Figure 2 presents the simulated $\text{PM}_{2.5}$ loadings from the CESM1 model, in terms of column burden and surface concentration, are significantly increasing throughout the 21st century. The increase in the total $\text{PM}_{2.5}$ is approximately 8% for the column burden and 2% for the surface concentration at the end of the 21st century (2090-2099) with respect to the current state (2006-2015). These increasing trends of $\text{PM}_{2.5}$ loadings are mainly due to the significant increases of the major $\text{PM}_{2.5}$ species, except for SOA, in which the surface concentration presents a slight decrease. Furthermore, the increases of all major $\text{PM}_{2.5}$ species in terms of column burden (BC: 11%, SO_4 : 6%, SOA: 11%, and POM: 11%) show stronger than the surface concentration (BC: 4%, SO_4 : 2%, SOA: -1%, and POM: 4%).

For comparison, we also evaluated the future changes of $\text{PM}_{2.5}$ concentrations and the associated species along the RCP8.5 forcing trajectory from the large ensemble simulations of CESM1 (Figure not shown). Different from changes of aerosol concentrations under the fixed aerosol simulations, the $\text{PM}_{2.5}$ concentrations and the associated species present uniformly decreasing trends across eastern China from the simulations along the RCP8.5 forcing. The decreasing trends in the RCP8.5 simulations are mainly attributed to the prescribed decrease of aerosol forcing in the

future in RCP database (Xu and Lin, 2017). The climate change induced by the GHG-warming might exacerbate the air pollution, but the impacts cannot compensate the prescribed decreasing trend of aerosol concentration.

As mentioned above, the PM_{2.5} surface concentration in the two economic zones of YRD and PRD present a negative response to the GHG-induced warming, while the corresponding column burden shows significantly increasing trends (Fig. S3). The decreases of the surface concentration over these two zones are primarily contributed by the changes of SO₄ and SOA, while there are no obvious trends for BC and POM (Figs. S4-S7). The robust response of the increased surface wind speed and decreased upper-level wind speed to GHG warming can be partly responsible for the changes of the major PM_{2.5} species in these two zones, which will be further discussed. Over the zones of JJJ and SCB, both the PM_{2.5} concentrations and the associated major PM_{2.5} species present the significantly rising trends throughout the 21st century. For the surface concentration, PM_{2.5} is reported to increase by 3% and 4% in the regions of JJJ and SCB, respectively, at the end of the 21st century. The BC is reported to increase by 4% and 8% for JJJ and SCB, respectively, ~~at the end of the 21st century.~~ The other species, such as SO₄ and POM, increase by 4% and 4%, respectively, in the JJJ regions and by 2% and 9%, respectively, in SCB regions. Relatively stronger responses can be seen in changes of the column burden for all major species (Figs. S4-S7). The increased concentrations of PM_{2.5} species finally result in significantly increasing trends of the total PM_{2.5} loading over these two regions, which will present a more direct effect on human health.

The increase in PM_{2.5} surface concentration throughout the 21st century substantially leads to the significant increase of the light anthropogenic PM_{2.5} pollution days (PM_{2.5} > 25 µg/m³) across the northwestern part of eastern China (Fig. S83). Due to the decrease of PM_{2.5} concentration over the southeastern part of eastern China, the light anthropogenic air pollution days can be expected to decrease in this region. Estimation shows that the number of the light air pollution days would be decreased by approximately 10 days at the end of the 21st century with respect to the early period of this century in the region. However, the annual mean light air pollution days is reported to increase averaged over the eastern China at the end of this century despite the aerosol emission is constant throughout the experiment. However, In contrast to the light air pollution days, the severe anthropogenic air pollution days (PM_{2.5} > 75 µg/m³) show a ~~robust position-positive~~ response to the GHG-induced warming across eastern China, particularly for the regions around JJJ in which the high PM_{2.5} concentration was localized (Fig. 3). The severe air pollution days is estimated to increase by more than 2 days at the end of this century when compared to the early period over this region. Considering the underestimation in aerosol concentration by CESM1 model in China, the percentile threshold metric is also applied here to estimate the future changes in light (90th) and severe (99th) air pollution days. Similar results can be obtained (Fig. S8). The increase of the severe anthropogenic air pollution days is considerably stronger than the light air pollution days, with an increase of approximately 68% to be observed at the end of 21st century, while an increase of 3% is expected for the light air pollution days over eastern China.

3.3 Attributable changes due to GHG warming

Although the aerosol emission was constant throughout the experiment, our study reveals that the PM_{2.5} loadings and their associated pollution days still present ~~significant~~ increases throughout the 21st century, primarily resulting from the impact of climate change induced by GHG warming. One may ask how large a contribution the climate change exerts on the changes in anthropogenic air pollution. To quantitatively address this issue, the framework of the “Fraction of Attributable Risk (FAR)” that has been widely used for attribute analyses of climate extreme changes (Chen and Sun, 2017; Stott et al., 2004) is employed in this study.

Figure 4 shows the percentage changes of the anthropogenic air pollution days throughout the 21st century over eastern China and their associated FAR variations. The regional averaged anthropogenic air pollution days present an ~~obvious~~ significant increase in the 21st century as addressed above. Correspondingly, synchronous increasing trends can be found in FAR for both light and severe anthropogenic air pollution days. For the light pollution days, FAR is estimated to be 28% at the end of the 21st century, implying that approximately 28% of the pollution days are contributed by the climate change that was induced by GHG warming. For the severe pollution days, FAR shows a relatively smaller value of approximately 11%. Furthermore, the high FAR values are mainly located over the regions of high PM_{2.5} loadings concentrated over eastern China, suggesting considerably stronger effects of climate changes in ~~this~~ these study regions. Note that the FAR values estimated in this research may be underestimated because the GHG-induced warming impact was

involved in the selected reference period that resulted in the overestimation of the probability of anthropogenic air pollution days.

3.4 Effects of the changes in meteorological conditions

We further examined the changes of meteorological conditions induced by the GHG warming that alternatively exerted effects on air pollution. Our results show that the local boundary layer height presents as higher under the warming scenario (Fig. 5a), which benefits the vertical transport of the air pollutant.

However, a robust negative response of the horizontal advection to the GHG-induced warming across eastern China can be found in the troposphere (Fig. 5b, c), facilitating air pollutant accumulation. The change of surface wind speed in response to the GHG warming is highly similar with the variation of PM_{2.5} surface concentration, with wind speed increasing in the southeastern part of eastern China and decreasing in the northwestern part. Variations of surface wind speeds are thus mainly responsible for the changes of PM_{2.5} surface concentration over eastern China. Different responses can be found for the tropospheric upper-level wind speeds, which are reported to substantially decrease. These decreases would directly result in significant increases of the stagnation days over eastern China, particularly over the northern region and SCB~~basin~~ (Fig. 6). The decreasing trend of wind speed in the 21st century across China not only exists in CEMS1 model, but also happens in the other global climate models that participated in Coupled Model Intercomparison Project Phase 3 (CMIP3) and CMIP5 (Jiang et al., 2010a; McInnes et al., 2011), as well as in regional climate models (Jiang et al., 2010b).

In response to the GHG-induced warming, the stagnation days over eastern China are estimated to increase by 6% at the end of 21st century with respect to the current period. For the specific economic zones, the stagnation days over the SCB and JJJ regions show considerably stronger rising trends, while relatively weaker increases are observed over the YRD and PRD regions. The number of stagnation days is estimated to increase by 13% and 6% at the end of the 21st century for the SCB and JJJ regions, respectively. Briefly, though the atmospheric stratification appears to be considerably more unstable in response to the GHG warming, the weakened horizontal advection would substantially increase the stagnation days over eastern China, which provides a beneficial background for the air pollutant accumulation and further increases the occurrence probability of the anthropogenic air pollution events.

Early studies have documented a significant increase in total precipitation across China due to the GHG-induced warming (Chen, 2013; Li et al., 2018; Wang et al., 2012), which seems to represent a conflict with the increase of the anthropogenic air pollution days. To resolve this issue, the precipitation changes in terms of light precipitation days (daily accumulated precipitation < 10 mm) and heavy precipitation days (> 10 mm) are further examined (Fig. 5d, e). Clearly, the heavy precipitation days present an increase, while the light precipitation days show a decrease, across eastern China in response to the warming. Though the precipitation shifts toward heavy precipitation events, its cleansing impact on air pollutants has not increased because an increase in heavy precipitation days appears to be insufficient to further enhance the wet removal ability (Xu and Lamarque, 2018). In contrast, the decrease in

light precipitation days substantially weakens the wet deposition of air pollutants, leading to the increase of the PM_{2.5} loading, as well as anthropogenic air pollution days. The future changes of precipitation days present much robust. Both the increasing trends of heavy precipitation days and the decreasing trends of light precipitation days are also obvious across China simulated by the CMIP5 models (Chen and Sun, 2013; 2018), as well as the regional climate models (Gao et al., 2012).

4. Conclusions

The world is predicted to experience increased disasters, such as heat waves, flash floods, and storms, due to the continuous global warming induced by the GHG increase. The research question we aim to address in this study is how the GHG warming would affect the anthropogenic PM_{2.5} pollutions across China. Our evaluations show that the anthropogenic PM_{2.5} loadings, as well as the anthropogenic PM_{2.5} pollution days, would ~~substantially~~ increase under the global warming conditions even the aerosol emissions fixed at current levels. More stringent regulations are thus suggested for regional aerosol emissions to maintain the air quality standard as the current state.

The climate changes induced by GHG warming exert their effects on the anthropogenic air pollutions across eastern China via two ways that are of interest in this study. First, the weakened tropospheric wind speed induced by the GHG warming would result in a decrease of the horizontal advection and lead to an increase in the number of stagnation days, facilitating the local accumulation of air pollutants. Second, the number of light precipitation days would decrease due to GHG-induced

warming, although the total precipitation would clearly increase across China. This shift toward more no-rainfall days would further weaken the wet deposition of PM_{2.5} pollutants. Thus, the increased stagnation days and decreased light precipitation days provide a beneficial background for the occurrence of anthropogenic air pollution. Of course, under the warming scenarios, a large discrepancy exists among the different meteorological processes that benefit the air pollutions at the current state, leading to the fuzzy recognition of air pollution change. For example, the boundary layer height shows an increase in response to the GHG warming that may strengthen the vertical dissipation of air pollutants. Thus, more studies are suggested in the future to further understand the mechanisms governing air quality across China.

Author contributions

H. P. Chen and H. J. Wang designed the research; H. P. Chen analyzed the data.

All the authors discussed the results and wrote the paper.

Competing interests

The authors declare that they have no conflict of interest.

Acknowledgements

This work is jointly supported by the National Natural Science Foundation of China (Grant No: 41421004), the National Key Research and Development Program of China (Grant No: 2016YFA0600701), and the CAS-PKU Joint Research Program.

References

- Cai, W. J., Li, K., Liao, H., Wang, H. J., and Wu, L. X.: Weather conditions conducive to Beijing severe haze more frequent under climate change, *Nature Climate Change*, 7, 257-263, 2017.
- Cao, C., Lee, X. H., Liu, S. D., Schultz, N., Xiao, W., Zhang, M., and Zhao, L.: Urban heat islands in China enhanced by haze pollution, *Nature Communications*, 7, 12509, 2016.
- Chen, H. P.: Projected change in extreme rainfall events in China by the end of the 21st century using CMIP5 models, *Chin. Sci. Bull.*, 58, 1462-1472, 2013.
- Chen, H. P., and Sun, J. Q.: Projected change in East Asian summer monsoon precipitation under RCP scenario, *Meteorol. Atmos. Phys.*, 121, 55-77, 2013.
- Chen, H. P. and Sun, J. Q.: Contribution of human influence to increased daily precipitation extremes over China, *Geophys. Res. Lett.*, 44, 2436-2444, 2017.
- Chen, H. P., and Sun, J. Q.: Projected changes in climate extremes in China in a 1.5 °C warmer world, *Int. J. Climatol.*, 38, 3607-3617, 2018.
- Chen, H. P. and Wang, H. J.: Haze days in North China and the associated atmospheric circulations based on daily visibility data from 1960 to 2012, *J. Geophys. Res. Atmos.*, 120, 5895-5909, 2015.
- Ding, Y. H. and Liu, Y. J.: Analysis of long-term variations of fog and haze in China in recent 50 years and their relations with atmospheric humidity, *Sci. China Earth Sci.*, 57, 36-46, 2014.
- Feng, J., Quan, J., Liao, H., Li, Y., and Zhao, X.: An air stagnation index to qualify

extreme haze events in northern China, J. Atmos. Sci.,
doi:10.1175/JAS-D-17-0354.1, 2018.

Gao, H. and Li, X.: Influences of El Niño Southern Oscillation events on haze frequency in eastern China during boreal winters, *Int. J. Climatol.*, 35, 2682-2688, 2015.

Gao, J. H., Woodward, A., Vardoulakis, S., Kovats, S., Wilkinson, P., Li, L. P., Xu, L., Li, J., Yang, J., Li, J., Cao, L., Liu, X. B., Wu, H. X., and Liu, Q. Y.: Haze, public health and mitigation measures in China: A review of the current evidence for further policy response, *Sci. Total Environ.*, 578, 148-157, 2017.

Gao, X. J., Shi, Y., Zhang, D., and Giorgi, F.: Climate change in China in the 21st
century as simulated by a high resolution regional climate model, Chin. Sci. Bull.,
57, 1188-1195, 2012.

Han, Z. Y., Zhou, B. T., Xu, Y., Wu, J., and Shi, Y.: Projected changes in haze pollution potential in China: an ensemble of regional climate model simulations, *Atmos. Chem. Phys.*, 17, 10109-10123, 2017.

Horton, D. E., Harshvardhan, and Diffenbaugh, N. S.: Response of air stagnation frequency to anthropogenically enhanced radiative forcing, *Environ. Res. Lett.*, 7, 044034, 2012.

Huang, Q., Cai, X., Song, Y., and Zhu, T.: Air stagnation in China (1985-2014):
Climatological mean features and trends, Atmos. Chem. Phys., 17, 7793-7805,
2017.

Huang, Q., Cai, X., Wang, J., Song, Y., and Zhu, T.: Climatological study of the

boundary-layer air stagnation index for China and its relationship with air pollution, Atmos. Chem. Phys., 18, 7573-7593, 2018.

Hurrell, J. W., Holland, M. M., Gent, P. R., Ghan, S., Kay, J. E., Kushner, P. J., Lamarque, J. F., Large, W. G., Lawrence, D., Lindsay, K., Lipscomb, W. H., Long, M. C., Mahowald, N., Marsh, D. R., Neale, R. B., Rasch, P., Vavrus, S., Vertenstein, M., Bader, D., Collins, W. D., Hack, J. J., Kiehl, J., Marshall, S.: The community earth system model: A framework for collaborative research, Bull. Amer. Meteorol. Soc., 94(9), 1339-1360, 2013.

Jiang, Y., Luo, Y., and Zhao, Z. C.: Projection of wind speed changes in China in the 21st century by climate models (in Chinese), Chin. J. Atmos. Sci., 34, 323-336, 2010a.

Jiang, Y., Luo, Y., Zhao, Z. C., Shi, Y., Xu, Y. L., and Zhu, J. H.: Projections of wind changes for 21st century in China by three regional climate models, Chin. Geogra. Sci., 20, 226-235, 2010b.

Jeong, J. I. and Park, R. J.: Winter monsoon variability and its impact on aerosol concentrations in East Asia, Environ. Pollution, 221, 285-292, 2017.

Kay, J. E., Deser, C., Phillips, A., Mai, A., Hannay, C., Strand, G., Arblaster, J. M., Bates, S. C., Danabasoglu, G., Edwards, J., Holland, M., Kushner, P., Lamarque, J. F., Lawrence, D., Lindsay, K., Middleton, A., Munoz, E., Neale, R., Oleson, K., Polvani, L., and Vertenstein, M.: The community earth system model (CESM) large ensemble project: A community resource for studying climate change in the presence of internal climate variability, Bull. Amer. Meteorol. Soc., 96(8),

1333-1349, 2015.

Lamarque, J. F., Kyle, P. P., Meinshausen, M., Riahi, K., Smith, S. J., van Vuuren, D. P., Conley, A. J., and Vitt, F.: Global and region evolution of short-lived radiatively-active gases and aerosols in the Representative Concentration Pathway, *Climatic Change*, 109(1), 191-212, 2011.

Li, H. X., Chen, H. P., Wang, H. J., and Yu, E. T.: Future precipitation changes over China under 1.5 °C and 2.0 °C global warming targets by using CORDEX regional climate models, *Sci. Total Environ.*, 640-641, 543-554, 2018.

Li, K., Liao, H., Zhu, J., and Moch, J. M.: Implications of RCP emissions on future PM2.5 air quality and direct radiative forcing over China, *J. Geophys. Res. Atmos.*, 121, 12985-13008, 2016.

Li, K., Liao, H., Cai, W. J., and Yang, Y.: Attribution of anthropogenic influence on atmospheric patterns conducive to recent most severe haze over eastern China, *Geophys. Res. Lett.*, 45, 2072-2081, 2018.

Li, Q., Zhang, R. H., and Wang, Y.: Interannual variation of the wintertime fog-haze days across central and eastern China and its relation with East Asian winter monsoon, *Int. J. Climatol.*, 36, 346-354, 2016.

Liao, H. and Chang, W. Y.: Integrated assessment of air quality and climate change for policy-making-highlights of IPCC AR5 and research challenges, *National Science Review*, 1(2), 176-179, 2014.

McInnes, K. L., Erwin, T. A., and Bathols, J. M.: Global climate model projected changes in 10 m wind speed and direction due to anthropogenic climate change,

464 [Atmos. Sci. Lett., 12, 325-333, 2011.](#)

465 State Council: *Air pollution prevention and control action plan*. Clean Air Alliance of

466 *China Rep.*, 20 pp., www.cleanairchina.org/product/6349.html, 2013.

467 Stott, P. A., Stone, D. A., and Allen, M. R.: Human contribution to the European

468 heatwave of 2003, *Nature*, 432, 610-614, 2004.

469 Tang, G. Q., Zhao, P. S., Wang, Y. H., Gao, W. K., Cheng, M. T., Xin, J. Y., Li, X., and

470 Wang, Y. S.: Mortality and air pollution in Beijing: the long-term relationship,

471 *Atmos. Environ.*, 150, 238-243, 2017.

472 Tie, X. X., Huang, R. J., Dai, W. T., Cao, J. J., Long, X., Su, X. L., Zhao, S. Y., Wang,

473 Q. Y., and Li, G. H.: Effect of heavy haze and aerosol pollution on rice and wheat

474 productions in China, *Sci. Rep.*, 6, 29612, 2016.

475 Wang, H. J.: On assessing haze attribution and control measures in China, *Atmos.*

476 *Oceanic Sci. Lett.*, 11(2), 120-122, 2018.

477 Wang, H. J. and Chen, H. P.: Understanding the recent trend of haze pollution in

478 eastern China: roles of climate change, *Atmos. Chem. Phys.*, 16, 4205-4211,

479 2016.

480 Wang, H. J., Chen, H. P., and Liu, J. P.: Arctic sea ice decline intensified haze

481 pollution in eastern China, *Atmos. Oceanic Sci. Lett.*, 8, 1-9, 2015.

482 Wang, H. J., Sun, J. Q., Chen, H. P., Zhu, Y. L., Zhang, Y., Jiang, D. B., Lang, X. M.,

483 Fan, K., Yu, E. T., and Yang, S.: Extreme climate in China: facts, simulation and

484 projection. *Meteorol. Z.*, 21, 279-304, 2012.

485 Wang, X., Dickinson, R., Su, L., Zhou, C., and Wang, K.: PM_{2.5} pollution in China

and how it has been exacerbated by terrain and meteorological conditions, Bull. Amer. Meteorol. Soc., 99(1), 105-119, 2018.

World Health Organization: *Air quality guidelines: Global update 2005*. World Health Organization Rep., 496 pp., www.euro.who.int/_data/assets/pdf_file/0005/78638/E90038.pdf/, 2014.

Xiao, D., Li, Y., Fan, S. J., Zhang, R. H., Sun, J. R., and Wang, Y.: Plausible influence of Atlantic Ocean SST anomalies on winter haze in China, Theor. Appl. Climatol., 122, 249-257, 2015.

Xu, Y. Y., and Lin, L.: Pattern scaling based projections for precipitation and potential evapotranspiration: sensitivity to composition of GHGs and aerosols forcing, Climatic Change, 140, 635-647, 2017.

Xu, Y. Y. and Lamarque, J. F.: Isolating the meteorological impact of 21st century GHG warming on the removal and atmospheric loading of anthropogenic fine particulate matter pollution at global scale, Earth's Future, 6, 428-440, 2018.

Yang, Y., Liao, H., and Lou, S. J.: Increase in winter haze over eastern China in recent decades: roles of variations in meteorological parameters and anthropogenic emissions, J. Geophys. Res. Atmos., 121, 13050-13065, 2016.

Yang, Y., Russell, L. M., Lou, S. J., Liao, H., Guo, J. P., Liu, Y., Singh, B., and Ghan, S. J.: Dust-wind interactions can intensify aerosol pollution over eastern China, Nature communications, 8, 15333, 2017a.

Yang, Y., Wang, H. L., Smith, S. J., Ma, P. L., and Rasch, P. J.: Source attribution of black carbon and its direct radiative forcing in China, Atmos. Chem. Phys., 17,

508 [4319-4336, 2017b.](#)

509 [Yang, Y., Wang, H. L., Smith, S. J., Easter, R., Ma, P. L., Qian, Y., Yu, H. B., Li, C.,](#)
510 [and Rasch, P. J.: Global source attribution of sulfate concentration and direct and](#)
511 [indirect radiative forcing, Atmos. Chem. Phys., 17, 8903-8922, 2017c.](#)

512 Yin, Z. C. and Wang, H. J.: The relationship between the subtropical Western Pacific
513 SST and haze over North-Central North China Plain, Int. J. Climatol., 36,
514 3479-3491, 2016.

515 Yin, Z. C., Wang, H. J., and Chen, H. P.: Understanding severe winter haze events in
516 the North China Plain in 2014: roles of climate anomalies, Atmos. Chem. Phys.,
517 17, 1641-1651, 2017.

518 Yin, Z. C., Wang, H. J., and Yuan, D. M.: Interdecadal increase of haze in winter over
519 North China and the Huang-huai area and the weakening of the East Asia winter
520 monsoon (in Chinese), Chin. Sci. Bull., 60, 1395-1400, 2015.

521 Zhang, R. H., Li, Q., and Zhang, R. N.: Meteorological conditions for the persistent
522 severe fog and haze event over eastern China in January 2013, Sci. China Earth
523 Sci., 57, 26-35, 2014.

524 Zhang, Y., Ding, A. J., Mao, H. T., Nie, W., Zhou, D. R., Liu, L. X., Huang, X., and Fu,
525 C. B.: Impact of synoptic weather patterns and inter-decadal climate variability
526 on air quality in the North China plain during 1980-2013, Atmos. Environ., 124,
527 119-128, 2016a.

528 Zhang, Z., Zhang, X., Goog, D., Kim, S., Mao, R., and Zhao, X.: Possible influence of
529 atmospheric circulations over winter haze pollution in the Beijing-Tian-Hebei

530 region, northern China, Atmos. Chem. Phys., 16, 561-571, 2016b.

531 Zhao, S., Li, J. P., and Sun, C.: Decadal variability in the occurrence of wintertime

532 haze in central eastern China tied to the Pacific Decadal Oscillation, Sci. Rep., 6,

533 27424, 2016.

534 Zhao, S. Y., Zhang, H., and Xie, B.: The effects of El Niño-Southern Oscillation on

535 the winter haze pollution of China, Atmos. Chem. Phys., 18, 1863-1877, 2018.

536

Figure captions

Figure 1. Observed PM_{2.5} pollution conditions over eastern China during the past years. (a) Annual averaged PM_{2.5} concentration ($\mu\text{g}/\text{m}^3$) for the years of 2015-2017. (b) Variations of annual averaged PM_{2.5} concentration (green bars) in Beijing city and the corresponding number of the severe PM_{2.5} pollution days (red bars). The severe pollution days are defined as the daily averaged PM_{2.5} concentration exceeding 75 $\mu\text{g}/\text{m}^3$. (c), (d), and (e) are similar to (b), but for the results of Shanghai, Guangzhou, and Chengdu city, respectively.

Figure 2. Plots of future changes of the total PM_{2.5} as well as its associated species averaged over eastern China in terms of the surface concentration ($\mu\text{g}/\text{m}^3$, right axis in red) and column burden (mg/m^2 , left axis in blue) from the simulations of the RCP8.5_FixAerosol2005 experiment. (a) PM_{2.5}, (b) BC, (c) SO₄, (d) POM, and (e) SOA. Ensemble variance (1 sigma) for surface concentration is shown in red shadings.

Figure 3. Changes of ~~severe~~the anthropogenic PM_{2.5} pollution days ($>75 \mu\text{g}/\text{m}^3$) across eastern China from the RCP8.5_FixAerosol2005 experiment. The top panel (a, b) shows the changes of light air pollution days ($> 25 \mu\text{g}/\text{m}^3$) and the bottom panel (c, d) shows the results of severe air pollution days ($> 75 \mu\text{g}/\text{m}^3$). The left panel (a, c) illustrates the annual averaged severe pollution days in 2006-2015 and the right panel (b, d) shows changes of the pollution days at the end of the 21st century with respect to 2006-2015. Dots in (b) and (d) mean the changes are significant at the 95% confidence level using Student T-test for all years and ensembles. Units: days.

Figure 4. Attributable changes of anthropogenic air pollution days to the increased greenhouse gases emissions. (a) Spatial distribution of FAR for the changes of severe PM_{2.5} pollutions ($> 75 \mu\text{g}/\text{m}^3$) at the end of the 21st century over eastern China. (b) Regional averaged relative changes of air pollution days (left axis in red; $> 25 \mu\text{g}/\text{m}^3$) and the corresponding variation of FAR (right axis in blue). Ensemble variance (1 sigma) for the relative changes of pollution days is shown in red shadings. (c) is similar to (b), but for the severe PM_{2.5} pollution days. Units: %.

Figure 5. Simulated changes in weather conditions of the air pollutions across eastern China due to the GHG-induced warming. (a) Changes of the planetary boundary layer height (PBLH) at the end of the 21st century with respect to the years of 2006-2015 from the RCP8.5_FixAerosol2005 experiment. (b) and (c) are similar to (a) but for the wind speed at near-surface and 500-hPa levels, respectively. (d) Changes in the light precipitation days (daily accumulated precipitation $< 10 \text{ mm}$) at the end of the 21st century with respect to the current state. (e) is similar to (d) but for the heavy precipitation days ($> 10 \text{ mm}$). Dots in the figure mean the changes are significant at the 95% confidence level using Student T-test for all years and ensembles. Units: %.

Figure 6. Changes in the stagnant conditions across China due to the GHG-induced warming. (a) Distribution of the relative changes of the stagnation days at the end of the 21st century against the current state (2006-2015). Dots mean the changes are significant at the 95% confidence level using Student T-test for all years and ensembles. (b) Variations of the regional averaged stagnation days over

581 eastern China. Ensemble variance (1 sigma) is shown in red shadings. (c), (d), (e), and
582 (f) are similar to (b), but for the results of four Chinese economic zones, i.e., JJJ, YRD,
583 PRD, and SCB. Units: %.

584

585

Figures

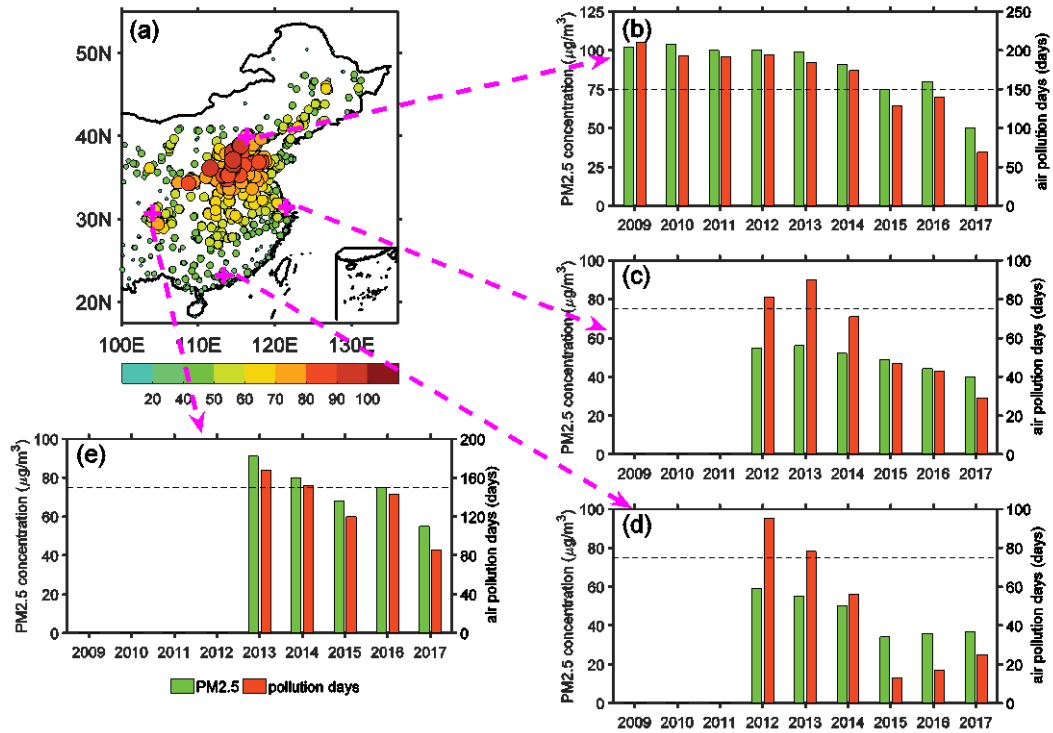


Figure 1. Observed PM_{2.5} pollution conditions over eastern China during the past years. (a) Annual averaged PM_{2.5} concentration ($\mu\text{g}/\text{m}^3$) for the years of 2015-2017. (b) Variations of annual averaged PM_{2.5} concentration (green bars) in Beijing city and the corresponding number of the severe PM_{2.5} pollution days (red bars). The severe pollution days are defined as the daily averaged PM_{2.5} concentration exceeding 75 $\mu\text{g}/\text{m}^3$. (c), (d), and (e) are similar to (b), but for the results of Shanghai, Guangzhou, and Chengdu city, respectively.

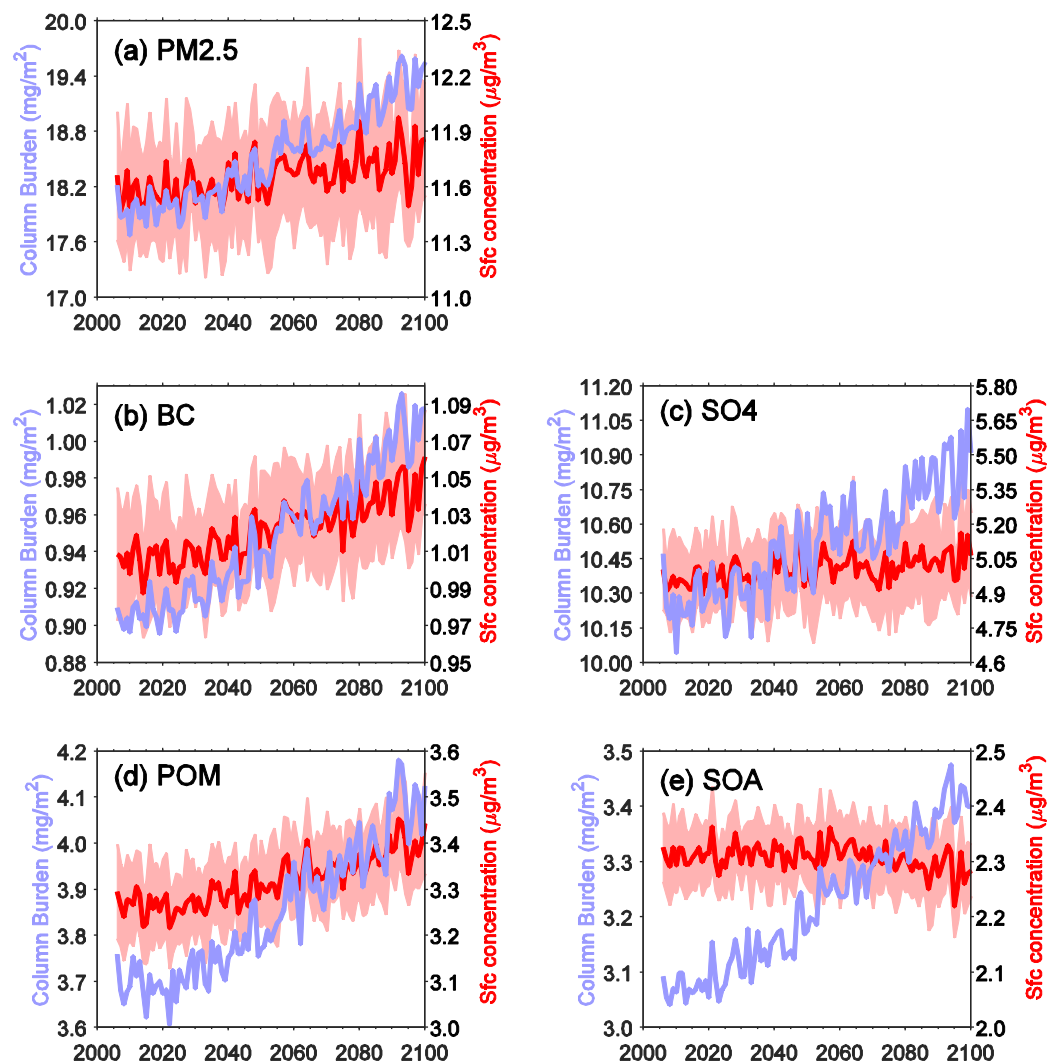
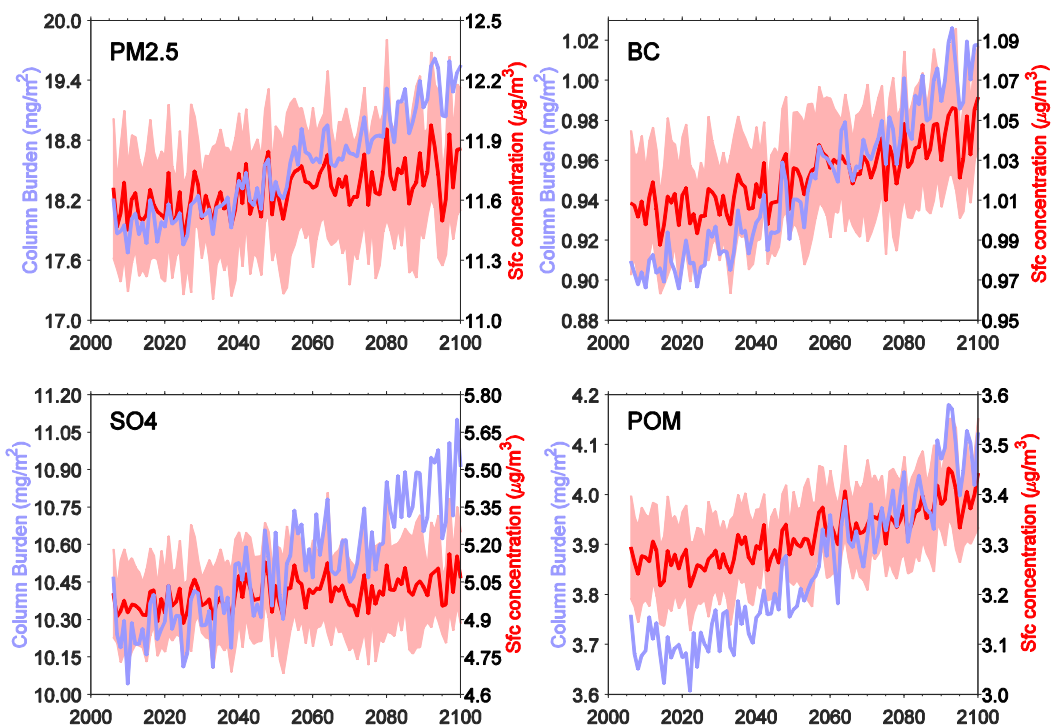


Figure 2. Plots of future changes of the total PM_{2.5} as well as its associated species averaged over eastern China in terms of the surface concentration ($\mu\text{g}/\text{m}^3$, right axis in red) and column burden (mg/m^2 , left axis in blue) from the simulations of the RCP8.5_FixAerosol2005 experiment. (a) PM_{2.5}, (b) BC, (c) SO₄, (d) POM, and (e) SOA. Ensemble variance (1 sigma) for surface concentration is shown in red shadings.

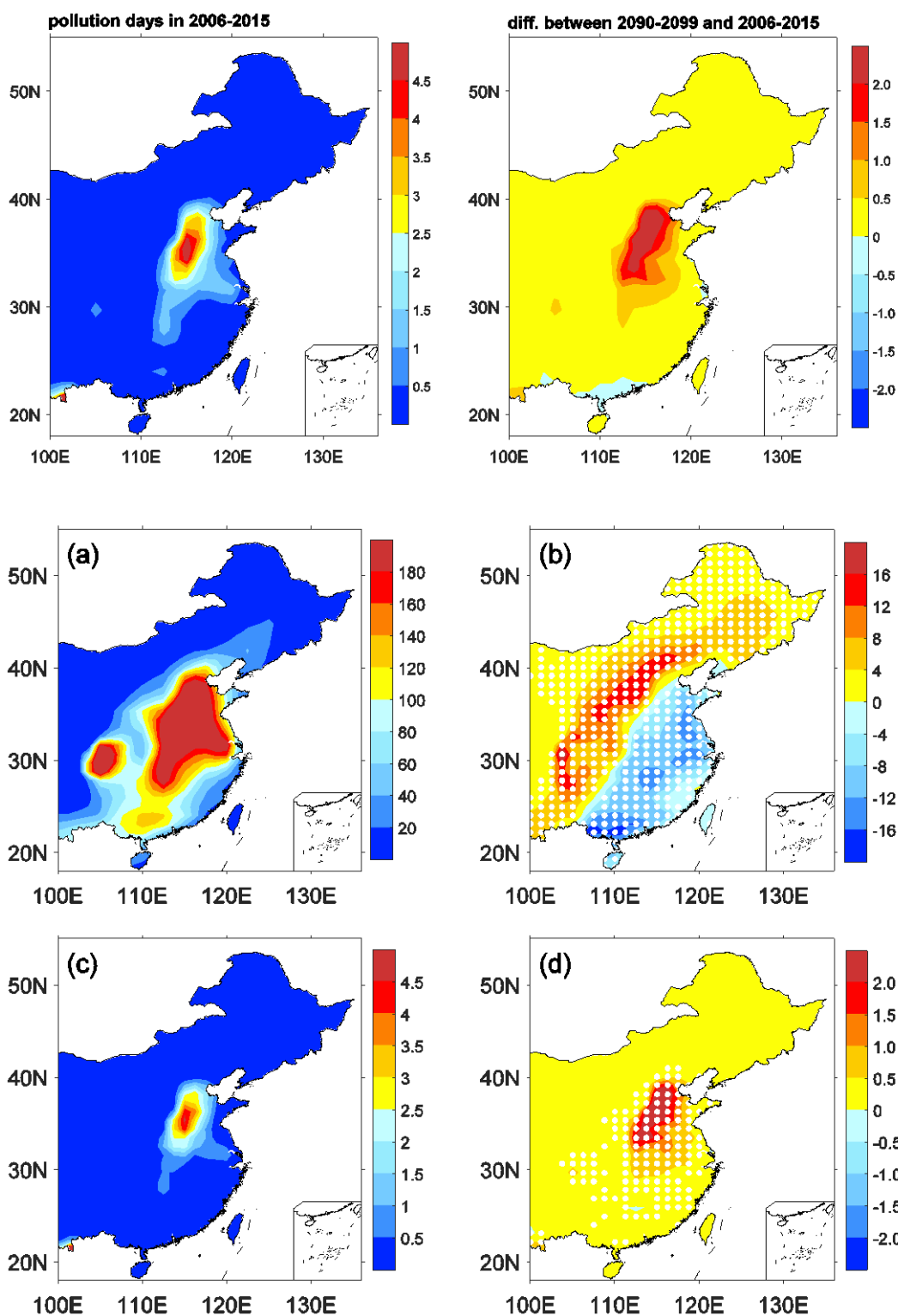


Figure 3. Changes of thesevere anthropogenic PM_{2.5} pollution days ($>75 \mu\text{g}/\text{m}^3$) across eastern China from the RCP8.5_FixAerosol2005 experiment. The top panel (a, b) shows the changes of light air pollution days ($> 25 \mu\text{g}/\text{m}^3$) and the bottom panel

(c, d) shows the results of severe air pollution days ($> 75 \mu\text{g}/\text{m}^3$). The left panel (a, c) illustrates the annual averaged severe pollution days in 2006-2015 and the right panel (b, d) shows changes of the pollution days at the end of the 21st century with respect to 2006-2015. Dots in (b) and (d) mean the changes are significant at the 95% confidence level using Student T-test for all years and ensembles. Units: days.

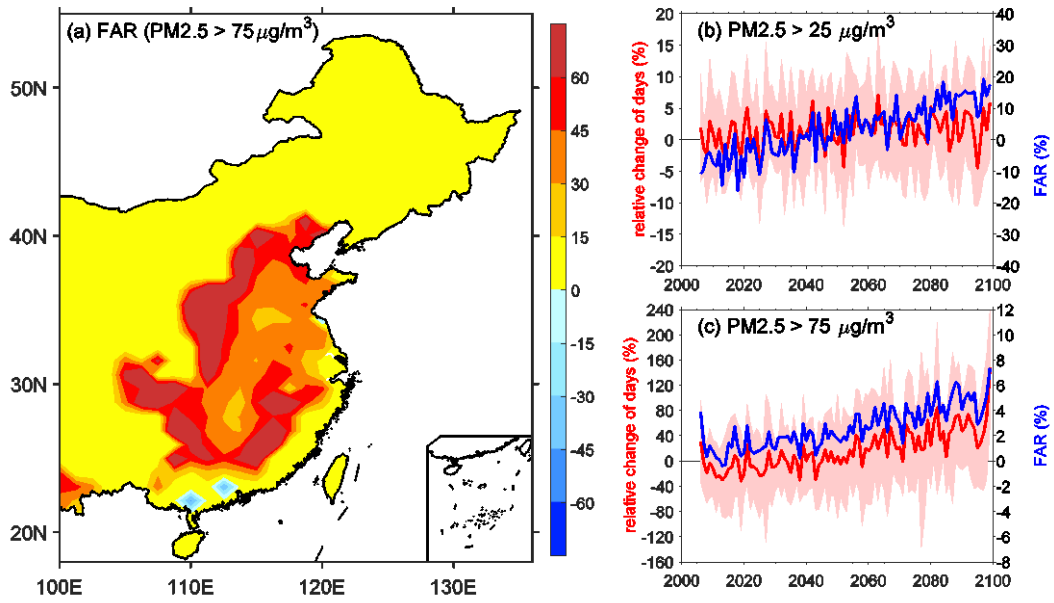
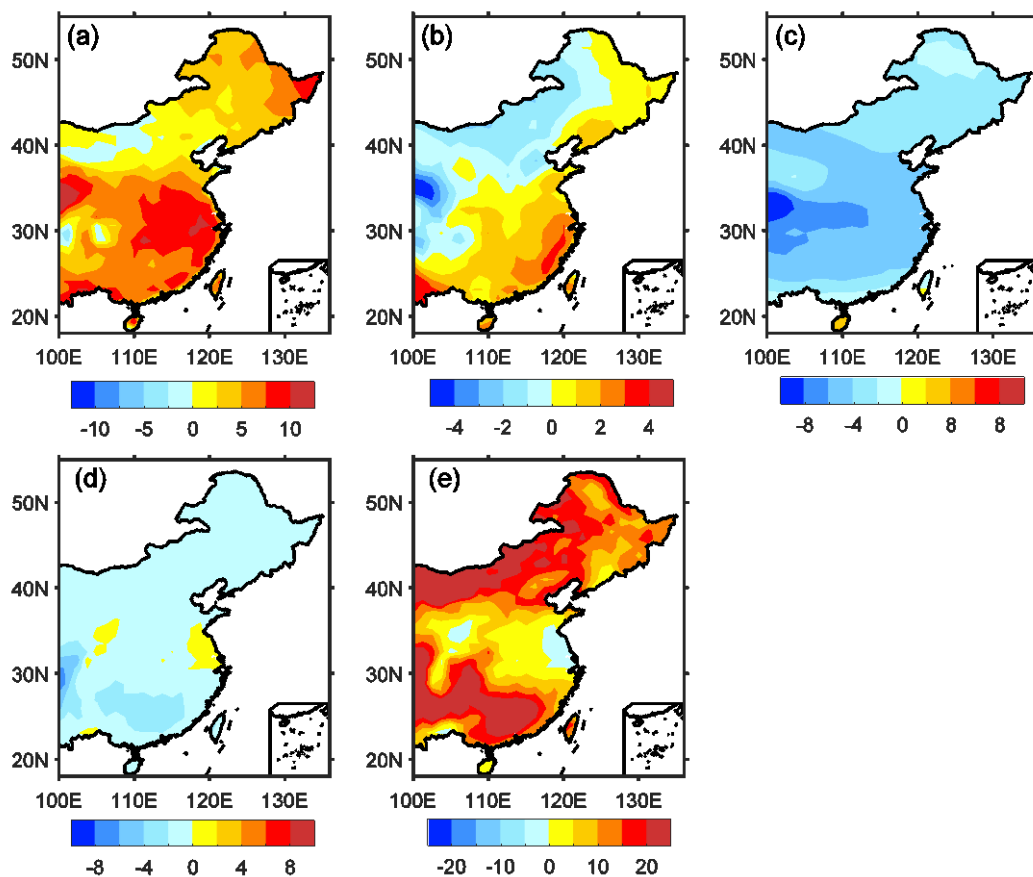
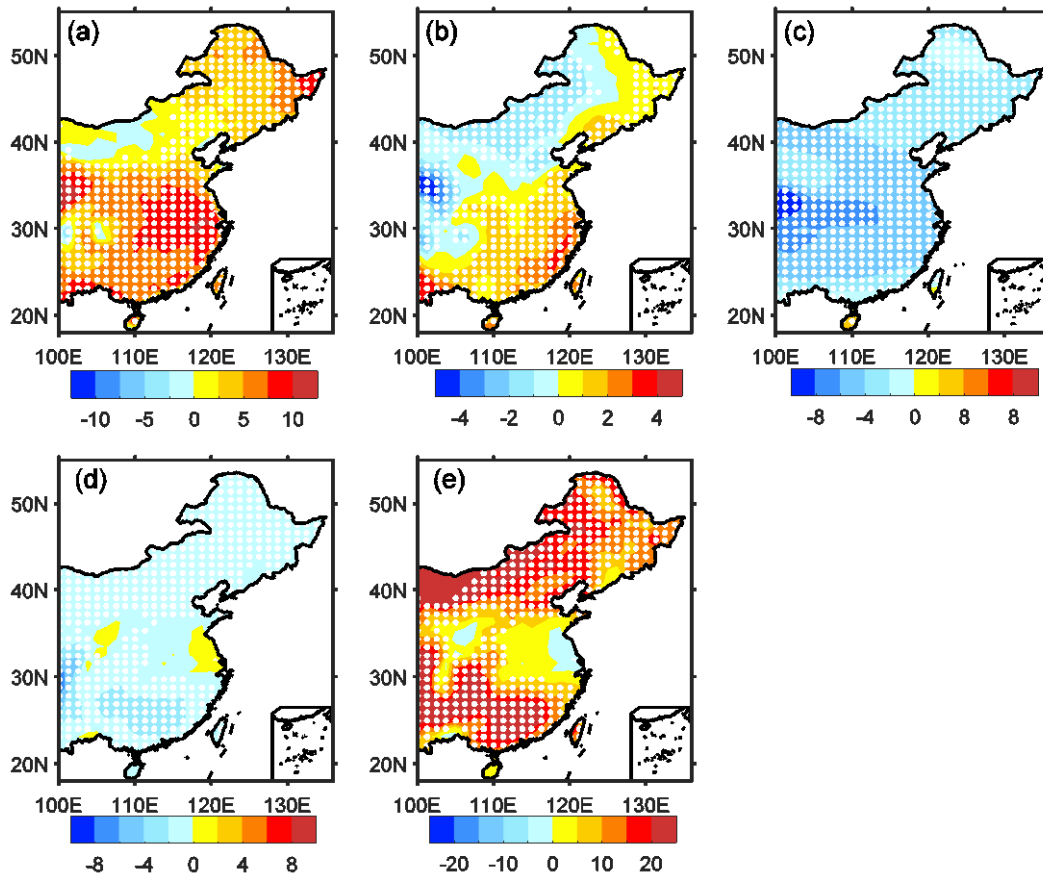


Figure 4. Attributable changes of anthropogenic air pollution days to the increased greenhouse gases emissions. (a) Spatial distribution of FAR for the changes of severe PM_{2.5} pollutions (> 75 µg/m³) at the end of the 21st century over eastern China. (b) Regional averaged relative changes of air pollution days (left axis in red; > 25 µg/m³) and the corresponding variation of FAR (right axis in blue). Ensemble variance (1 sigma) for the relative changes of pollution days is shown in red shadings. (c) is similar to (b), but for the severe PM_{2.5} pollution days. Units: %.



629



630

Figure 5. Simulated changes in weather conditions of the air pollutions across eastern China due to the GHG-induced warming. (a) Changes of the planetary boundary layer height (PBLH) at the end of the 21st century with respect to the years of 2006-2015 from the RCP8.5_FixAerosol2005 experiment. (b) and (c) are similar to (a) but for the wind speed at near-surface and 500-hPa levels, respectively. (d) Changes in the light precipitation days (daily accumulated precipitation < 10 mm) at the end of the 21st century with respect to the current state. (e) is similar to (d) but for the heavy precipitation days (> 10 mm). Dots in the figure mean the changes are significant at the 95% confidence level using Student T-test for all years and ensembles. Units: %.

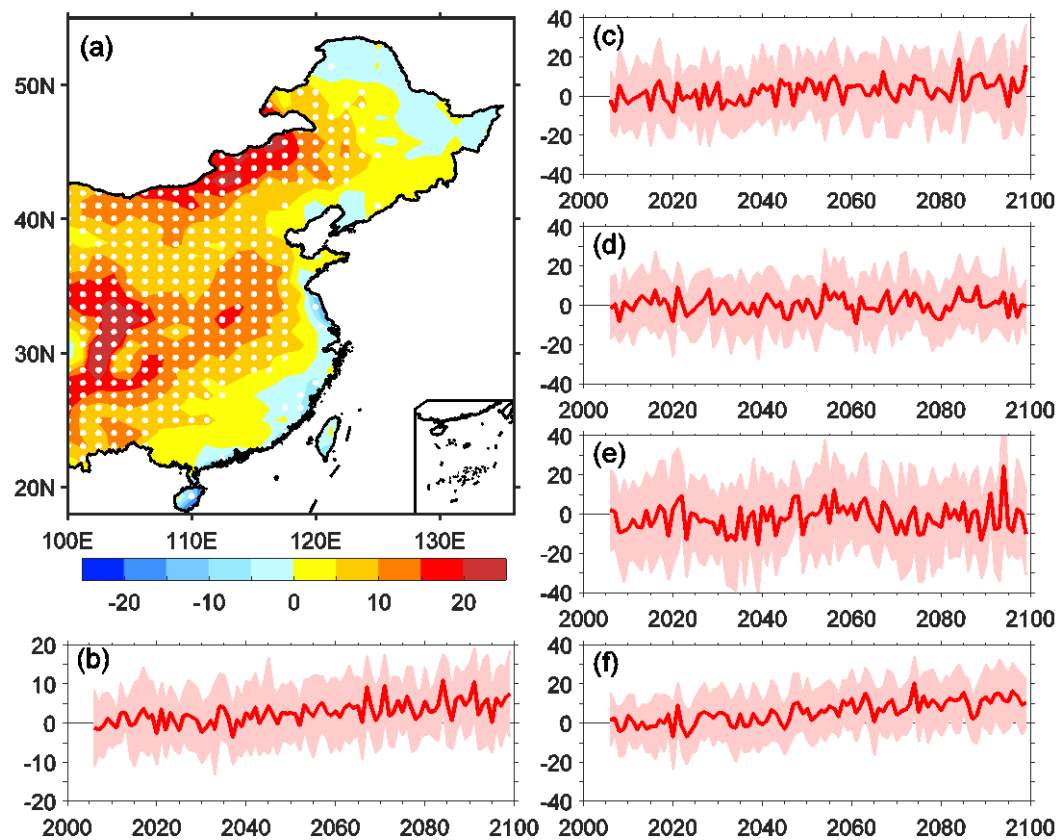
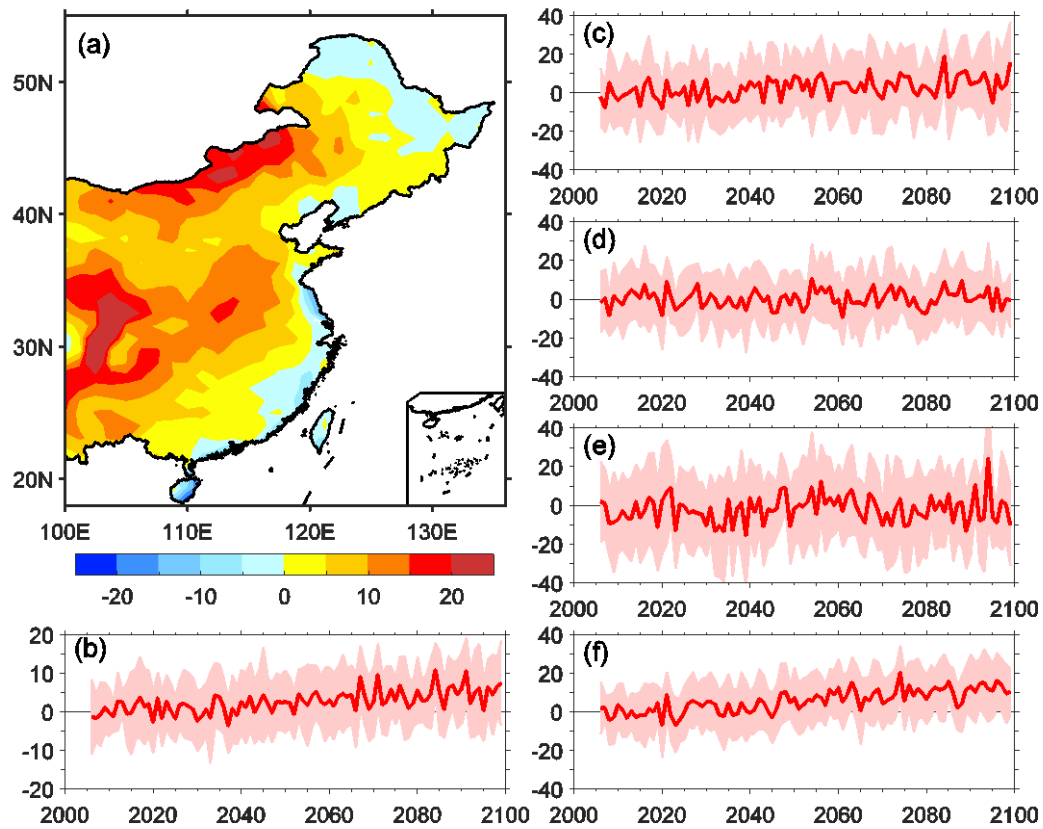


Figure 6. Changes in the stagnant conditions across China due to the

GHG-induced warming. (a) Distribution of the relative changes of the stagnation days at the end of the 21st century against the current state (2006-2015). Dots mean the changes are significant at the 95% confidence level using Student T-test for all years and ensembles. (b) Variations of the regional averaged stagnation days over eastern China. Ensemble variance (1 sigma) is shown in red shadings. (c), (d), (e), and (f) are similar to (b), but for the results of four Chinese economic zones, i.e., JJJ, YRD, PRD, and SCB. Units: %.

**Anthropogenic Fine Particulate Matter Pollution Will Be Exacerbated in Eastern
China Due to 21st-Century GHG Warming**

Huopo Chen^{1,2*}, Huijun Wang^{2,1}, Jianqi Sun^{1,2}, Yangyang Xu³, and Zhicong Yin²

¹ *Nansen-Zhu International Research Centre, Institute of Atmospheric Physics,
Chinese Academy of Sciences, Beijing, China*

² *Collaborative Innovation Center on Forecast and Evaluation of Meteorological
Disasters, Nanjing University for Information Science and Technology, Nanjing,
China*

³ *Department of Atmospheric Sciences, Texas A&M University, College Station Texas,
USA*

Corresponding author: Huopo Chen (chenhuopo@mail.iap.ac.cn)

Address: Nansen-Zhu International Research Centre, Institute of Atmospheric
Physics, Chinese Academy of Sciences, PO Box 9804, Beijing 100029,
China

Email: chenhuopo@mail.iap.ac.cn

Tel: (+86)010-82995057

Abstract

China has experienced a substantial increase in severe haze events over the past several decades, which is primarily attributed to the increased pollutant emissions caused by its rapid economic development. The climate changes observed under the warming scenarios, especially those induced by increases in greenhouse gases (GHG), are also conducive to the increase in air pollution. However, how the air pollution changes in response to the GHG warming has not been thoroughly elucidated to date. We investigate this change using the century-long large ensemble simulations with the Community Earth System Model 1 (CESM1) with the fixed anthropogenic emissions at the year 2005. Our results show that although the aerosol emission is assumed to be a constant throughout the experiment, anthropogenic air pollution presents positive responses to the GHG-induced warming. The anthropogenic PM_{2.5} concentration is estimated to increase averaged over eastern China at the end of this century, but varying from regions, with an increase over northwestern part of eastern China and a decrease over southeastern part. Similar changes can be observed for the light air pollution days. However, the severe air pollution days is reported to increase across eastern China at the end of this century, particularly around the Jing-Jin-Ji region. Further research indicates that the increased stagnation days and the decreased light precipitation days are the possible causes of the increase in PM_{2.5} concentration, as well as the anthropogenic air pollution days. Estimation shows that the effect of climate change induced by the GHG warming can account for 11%-28% of the changes in anthropogenic air pollution days over eastern China. Therefore, in the

41 future, more stringent regulations on regional air pollution emissions are needed to
42 balance the effect from climate change.
43

1. Introduction

The extraordinarily rapid development of China has caused extremely high aerosol loading and gaseous pollutant emissions that have enveloped most regions across China in the recent decades. The increased pollutant emissions, particularly for the particulate matter finer than 2.5 μm in aerodynamic diameter ($\text{PM}_{2.5}$), generally result in severe haze events and present a major threat to public health (Gao et al., 2017; Tang et al., 2017; Wang, 2018), crop production (Tie et al., 2016), and regional climates (Cao et al., 2016). For example, the annual averaged $\text{PM}_{2.5}$ in Beijing exceeded 75 $\mu\text{g}/\text{m}^3$ during 2009-2016 (Fig. 1b), which more than three times the recommended 24-hour standard (25 $\mu\text{g}/\text{m}^3$) of the World Health Organization (WHO). This degeneration of the air pollution across China, which is similar to that in Beijing, is primarily caused by the integrated effects of high emissions and poor ventilation (Chen and Wang, 2015; Zhang et al., 2016a). Many efforts are thus underway to reduce emissions that cause severe haze pollutions. However, the question remains of whether climate change will offset or facilitate these efforts.

Recent studies have documented that the exacerbation of air quality over eastern China was partly modulated by meteorological conditions and climate variability that are generally conducive to the severe haze occurrences (Li et al., 2018; Liao and Chang, 2014; Wang and Chen, 2016; Yang et al., 2016; Zhang et al., 2014; Zhang et al., 2016b). Specifically, Wang *et al.* (2015) revealed that the shrinking Arctic sea ice favors less cyclone activity and a more stable atmosphere conducive to haze formation, which can explain approximately 45%-67% of the interannual to

interdecadal variability of winter haze days over eastern China. Besides Arctic sea ice, other decadal variability and changes, including weak East Asian winter monsoon (Jeong et al., 2017; Li et al., 2016; Yin et al., 2015), strong El Niño-Southern oscillation (Gao and Li, 2015; Zhao et al., 2018), high Pacific decadal oscillation (Zhao et al., 2016), and high Arctic oscillation (Cai et al., 2017), may have contributed. In addition, the increasing winter haze days over eastern China may also be linked to the low boundary layer height (Huang et al., 2018; Wang et al., 2018), weakened northerly winds (Yang et al., 2017a), decreased relative humidity (Ding and Liu, 2014), and increased sea surface temperature (Xiao et al., 2015; Yin and Wang, 2016; Yin et al., 2017).

Global warming generally presents an adverse impact on the haze pollution across China. Simulations of the dynamic downscaling by the regional climate model RegCM4 under the RCP4.5 (Representative Concentration Pathway) scenarios have shown that the air environment carrying capacity tends to decrease, and the weak ventilation days tend to increase, in the 21st century across China, suggesting an increase in the haze pollution potential compared to the current state (Han et al., 2017). Furthermore, Cai *et al.* (2017) projected that the days conducive to severe haze pollution in Beijing would increase by 50% at the end of the 21st century (2050-2099) under the RCP8.5 scenarios compared to the historical period.

These qualitative estimations of the haze pollution response to climate changes generally derived from the *potential* changes of the corresponding meteorological conditions indirectly. No studies to date quantitatively assessed the simulated PM

directly. How the fine particulate matter pollution changes in response to the global warming in China has not been thoroughly elucidated to date. This study particularly focuses on the anthropogenic PM_{2.5} loading and its response to the future warming. In this study, the large ensemble simulations from the Community Earth System Model Version 1 (CESM1) throughout the 21st century that are induced by increasing greenhouse gases (GHG) emissions along the trajectory RCP8.5 but retaining the emissions of aerosols and/or their precursors fixed at the year of 2005 level (RCP8.5_FixAerosol2005; Xu and Lamarque, 2018) will be utilized.

2. Data and methods

2.1 PM_{2.5} observational datasets

Surface hourly PM_{2.5} concentration data released since 2013 are taken from the website of the Ministry of Environmental Protection (<http://106.37.208.233:20035>), which covers 1602 sites across China. The duration of available datasets varies across sites because of the gradual development of the monitoring network in recent years. In our study region of eastern China (east to 100 °E), there are 1263 sites remaining after the sites with missing values were removed during 2015-2017. Additionally, surface daily PM_{2.5} concentrations for the Beijing, Shanghai, Guangzhou, and Chengdu cities that had relatively longer monitoring times are also collected from the U.S. Beijing Embassy (<http://www.stateair.net/web/historical/1/1.html>).

2.2 CESM1 model simulations

The CESM1 is an Earth system model involving the atmosphere, land, ocean,

and sea-ice components with a nominal 1° by 1° horizontal resolution (Hurrell et al., 2013). The RCP8.5_FixAerosol2005 simulations are forced by the RCP8.5 scenario, but all emissions of sulfate (SO_4), black carbon (BC) and primary organic matter (POM), and secondary organic aerosols (SOA; or their precursors) and atmospheric oxidants are fixed at the present-day level (2005). These simulations include 16 ensemble members, differing solely in their atmospheric initial conditions with a tiny random temperature difference (order of 10^{-14}°C ; Kay et al., 2015). For comparison, the CESM1 large ensemble consists of 35-member simulations that forced by the RCP8.5 scenario are also employed here. Using these relatively large ensembles can substantially reduce the contribution of natural variability of the climate system to the result estimation (Xu and Lamarque, 2018).

For the aerosol emission in the RCP scenarios database, just its decadal change is considered rather than the emission at a single year (Lamarque et al., 2011). Here, the years of 2006-2015 are considered as the reference period in the RCP8.5_FixAerosol2005 simulations. The differences of the mean climates from the reference period are largely due to the increase in GHG emissions and are not attributed to the decline in aerosol emissions, as specified in RCP8.5. The changes of anthropogenic $\text{PM}_{2.5}$ loadings and anthropogenic air pollution days in our study are thus only a result of the GHG-induced climate change, rather than changes in aerosol emission. Note that just four species of $\text{PM}_{2.5}$ components that show a substantial threat to public health are considered here for analysis, including SO_4 , BC, POM, and SOA from the CESM1 simulations.

2.3 Definition of the fraction of attributable risk

The influences of the GHG-induced climate changes on the anthropogenic air pollutions in China are investigated using the metric of the fraction of attributable risk (FAR), which has been widely used for attribute analyses of climate extreme changes (Chen and Sun, 2017; Stott et al., 2004). FAR is defined as the $1-P_0/P_I$, where P_0 is the probability of exceeding a certain threshold during the reference period and P_I is the probability exceeding the same threshold during a given period. FAR thus presents the quantitative estimations of effects of the GHG-induced climate changes on the anthropogenic air pollutions.

2.4 Definition of stagnation days

The changes of the stagnation days that were induced by the increase of GHG emissions are also evaluated in our study to explore the possible impact of climate change on the anthropogenic air pollutions. The day is considered to be stagnant when the daily mean near-surface wind speed is less than 3.2 m/s, the daily mean 500-hPa wind speed is less than 13 m/s, and the daily accumulated precipitation is less than 1 mm (Horton et al., 2012). Early studies have suggested that this air stagnation definition might not be applicable for China to represent the air pollution condition under the seasonal scales (Feng et al., 2018; Wang et al., 2018). However, the annual mean stagnation generally presents good agreement with that of air pollution across China (Huang et al., 2017; 2018). The changes in the annual mean states of air stagnations over China at the end of 21st century will thus be discussed in the following.

3. Results

3.1 Observational changes in PM_{2.5} pollutions

The days of severe haze pollution increased over the past several decades across eastern China, particularly for the episodes of January 2013, December 2015, and December 2016, when several severe haze alerts were reached. High PM_{2.5} loading was centralized over the Jing-Jin-Ji (JJJ) region, Shangdong, and Henan provinces, as well as the Sichuan Basin (SCB, Fig. 1a). The annual mean PM_{2.5} mass concentrations for most sites over these regions exceed 75 $\mu\text{g}/\text{m}^3$. According to the statistics, there are approximately 95% sites where the annual mean PM_{2.5} concentration exceeded the WHO recommended 24-hour standard (25 $\mu\text{g}/\text{m}^3$) across eastern China, and there are 65 sites centralized by Beijing, where the annual mean PM_{2.5} concentration was larger than 75 $\mu\text{g}/\text{m}^3$, which would present the possibility of exposing people to serious health hazards (World Health Organization, 2014).

Regarding the four economic zones of Beijing, Shanghai, Guangzhou, and Chengdu cities over China, serious PM_{2.5} pollution can be expected in recent years, especially for the Beijing and Chengdu regions (Fig. 1). Taking Beijing as an example, the annual mean PM_{2.5} concentration was stably exceeding 100 $\mu\text{g}/\text{m}^3$, and more than a half of the year had experienced severe air pollution ($> 75 \mu\text{g}/\text{m}^3$) before 2013. Since 2013, China's State Council released its Air Pollution Prevention and Control Action Plan, which requires the key regions, including the JJJ, the Yangtze River Delta (YRD), and the Pearl River Delta (PRD) to reduce their atmospheric levels of PM_{2.5} by 25%, 20%, and 15%, respectively, by the end of year 2017 (State Council,

2013). Effort is obvious, and the $\text{PM}_{2.5}$ loading and the air pollution days present sharp decreases in recent years. However, the strict emission policies substantially cost the economic development, which cannot meet the current requirement of the rapid development of China. Thus, scientifically quantifying the roles of anthropogenic emissions and climate changes shows great importance for seeking the balance between socioeconomic development and emission reduction.

3.2 Simulated changes in anthropogenic $\text{PM}_{2.5}$ pollutions

A strong spatial correlation (0.69) is found for the annual mean $\text{PM}_{2.5}$ concentration between the site observation and median ensemble of CESM1 simulations over eastern China (Fig. S1). The high concentrations across eastern China, including the regions centralized by Beijing and Chengdu, are reasonably reproduced. However, a negative bias is obvious. Early studies (Li et al., 2016; Yang et al., 2017b; c) have documented that this low bias of aerosol concentration simulated by models is much more complicated in China and the causes mainly involve the uncertainties from aerosol emission amount, emission injection height, lack of nitrate, aerosol treatment in model as well as the coarse model resolution.

The median ensemble-mean change of the $\text{PM}_{2.5}$ surface concentration presents strong regional dependence across China with significantly decreasing trends over the southeastern part of eastern China and significantly increasing trends over the other regions throughout the 21st century (Fig. S2), even though the emissions are constant throughout the experiment. The regional differences in the total $\text{PM}_{2.5}$ changes are mainly due to SO_4 , which can account for approximately 50% of the total $\text{PM}_{2.5}$ mass

(Xu and Lamarque, 2018). The species of BC and POM are reported to significantly increase in the 21st century across eastern China, although the aerosol emissions were fixed at the level in 2005. Figure 2 presents the simulated PM_{2.5} loadings from the CESM1 model, in terms of column burden and surface concentration, are significantly increasing throughout the 21st century. The increase in the total PM_{2.5} is approximately 8% for the column burden and 2% for the surface concentration at the end of the 21st century (2090-2099) with respect to the current state (2006-2015). These increasing trends of PM_{2.5} loadings are mainly due to the significant increases of the major PM_{2.5} species, except for SOA, in which the surface concentration presents a slight decrease. Furthermore, the increases of all major PM_{2.5} species in terms of column burden (BC: 11%, SO₄: 6%, SOA: 11%, and POM: 11%) show stronger than the surface concentration (BC: 4%, SO₄: 2%, SOA: -1%, and POM: 4%).

For comparison, we also evaluated the future changes of PM_{2.5} concentrations and the associated species along the RCP8.5 forcing trajectory from the large ensemble simulations of CESM1 (Figure not shown). Different from changes of aerosol concentrations under the fixed aerosol simulations, the PM_{2.5} concentrations and the associated species present uniformly decreasing trends across eastern China from the simulations along the RCP8.5 forcing. The decreasing trends in the RCP8.5 simulations are mainly attributed to the prescribed decrease of aerosol forcing in the future in RCP database (Xu and Lin, 2017). The climate change induced by the GHG-warming might exacerbate the air pollution, but the impacts cannot compensate

the prescribed decreasing trend of aerosol concentration.

As mentioned above, the PM_{2.5} surface concentration in the two economic zones of YRD and PRD present a negative response to the GHG-induced warming, while the corresponding column burden shows significantly increasing trends (Fig. S3). The decreases of the surface concentration over these two zones are primarily contributed by the changes of SO₄ and SOA, while there are no obvious trends for BC and POM (Figs. S4-S7). The robust response of the increased surface wind speed and decreased upper-level wind speed to GHG warming can be partly responsible for the changes of the major PM_{2.5} species in these two zones, which will be further discussed. Over the zones of JJJ and SCB, both the PM_{2.5} concentrations and the associated major PM_{2.5} species present the significantly rising trends throughout the 21st century. For the surface concentration, PM_{2.5} is reported to increase by 3% and 4% in the regions of JJJ and SCB, respectively, at the end of the 21st century. The BC is reported to increase by 4% and 8% for JJJ and SCB, respectively. The other species, such as SO₄ and POM, increase by 4% and 4%, respectively, in the JJJ regions and by 2% and 9%, respectively, in SCB regions. Relatively stronger responses can be seen in changes of the column burden for all major species (Figs. S4-S7). The increased concentrations of PM_{2.5} species finally result in significantly increasing trends of the total PM_{2.5} loading over these two regions, which will present a more direct effect on human health.

The increase in PM_{2.5} surface concentration throughout the 21st century substantially leads to the significant increase of the light anthropogenic PM_{2.5}

pollution days ($\text{PM}_{2.5} > 25 \mu\text{g}/\text{m}^3$) across the northwestern part of eastern China (Fig. 3). Due to the decrease of $\text{PM}_{2.5}$ concentration over the southeastern part of eastern China, the light anthropogenic air pollution days can be expected to decrease in this region. Estimation shows that the number of the light air pollution days would be decreased by approximately 10 days at the end of the 21st century with respect to the early period of this century in the region. However, the annual mean light air pollution days is reported to increase averaged over the eastern China at the end of this century despite the aerosol emission is constant throughout the experiment. In contrast to the light air pollution days, the severe anthropogenic air pollution days ($\text{PM}_{2.5} > 75 \mu\text{g}/\text{m}^3$) show a positive response to the GHG-induced warming across eastern China, particularly for the regions around JJJ in which the high $\text{PM}_{2.5}$ concentration was localized (Fig. 3). The severe air pollution days is estimated to increase by more than 2 days at the end of this century when compared to the early period over this region. Considering the underestimation in aerosol concentration by CESM1 model in China, the percentile threshold metric is also applied here to estimate the future changes in light (90th) and severe (99th) air pollution days. Similar results can be obtained (Fig. S8).

3.3 Attributable changes due to GHG warming

Although the aerosol emission was constant throughout the experiment, our study reveals that the $\text{PM}_{2.5}$ loadings and their associated pollution days still present increases throughout the 21st century, primarily resulting from the impact of climate change induced by GHG warming. One may ask how large a contribution the climate

change exerts on the changes in anthropogenic air pollution. To quantitatively address this issue, the framework of the “Fraction of Attributable Risk (FAR)” that has been widely used for attribute analyses of climate extreme changes (Chen and Sun, 2017; Stott et al., 2004) is employed in this study.

Figure 4 shows the percentage changes of the anthropogenic air pollution days throughout the 21st century over eastern China and their associated FAR variations. The regional averaged anthropogenic air pollution days present an obvious increase in the 21st century as addressed above. Correspondingly, synchronous increasing trends can be found in FAR for both light and severe anthropogenic air pollution days. For the light pollution days, FAR is estimated to be 28% at the end of the 21st century, implying that approximately 28% of the pollution days are contributed by the climate change that was induced by GHG warming. For the severe pollution days, FAR shows a relatively smaller value of approximately 11%. Furthermore, the high FAR values are mainly located over the regions of high PM_{2.5} loadings concentrated over eastern China, suggesting considerably stronger effects of climate changes in these regions. Note that the FAR values estimated in this research may be underestimated because the GHG-induced warming impact was involved in the selected reference period that resulted in the overestimation of the probability of anthropogenic air pollution days.

3.4 Effects of the changes in meteorological conditions

We further examined the changes of meteorological conditions induced by the GHG warming that alternatively exerted effects on air pollution. Our results show that the local boundary layer height presents as higher under the warming scenario (Fig.

5a), which benefits the vertical transport of the air pollutant.

However, a robust negative response of the horizontal advection to the GHG-induced warming across eastern China can be found in the troposphere (Fig. 5b, c), facilitating air pollutant accumulation. The change of surface wind speed in response to the GHG warming is highly similar with the variation of PM_{2.5} surface concentration, with wind speed increasing in the southeastern part of eastern China and decreasing in the northwestern part. Variations of surface wind speeds are thus mainly responsible for the changes of PM_{2.5} surface concentration over eastern China. Different responses can be found for the tropospheric upper-level wind speeds, which are reported to substantially decrease. These decreases would directly result in significant increases of the stagnation days over eastern China, particularly over the northern region and SCB (Fig. 6). The decreasing trend of wind speed in the 21st century across China not only exists in CEMS1 model, but also happens in the other global climate models that participated in Coupled Model Intercomparison Project Phase 3 (CMIP3) and CMIP5 (Jiang et al., 2010a; McInnes et al., 2011), as well as in regional climate models (Jiang et al., 2010b).

In response to the GHG-induced warming, the stagnation days over eastern China are estimated to increase by 6% at the end of 21st century with respect to the current period. For the specific economic zones, the stagnation days over the SCB and JJJ regions show considerably stronger rising trends, while relatively weaker increases are observed over the YRD and PRD regions. The number of stagnation days is estimated to increase by 13% and 6% at the end of the 21st century for the SCB and

307 JJJ regions, respectively. Briefly, though the atmospheric stratification appears to be
308 considerably more unstable in response to the GHG warming, the weakened
309 horizontal advection would substantially increase the stagnation days over eastern
310 China, which provides a beneficial background for the air pollutant accumulation and
311 further increases the occurrence probability of the anthropogenic air pollution events.

312 Early studies have documented a significant increase in total precipitation across
313 China due to the GHG-induced warming (Chen, 2013; Li et al., 2018; Wang et al.,
314 2012), which seems to represent a conflict with the increase of the anthropogenic air
315 pollution days. To resolve this issue, the precipitation changes in terms of light
316 precipitation days (daily accumulated precipitation < 10 mm) and heavy precipitation
317 days (> 10 mm) are further examined (Fig. 5d, e). Clearly, the heavy precipitation
318 days present an increase, while the light precipitation days show a decrease, across
319 eastern China in response to the warming. Though the precipitation shifts toward
320 heavy precipitation events, its cleansing impact on air pollutants has not increased
321 because an increase in heavy precipitation days appears to be insufficient to further
322 enhance the wet removal ability (Xu and Lamarque, 2018). In contrast, the decrease in
323 light precipitation days substantially weakens the wet deposition of air pollutants,
324 leading to the increase of the $PM_{2.5}$ loading, as well as anthropogenic air pollution
325 days. The future changes of precipitation days present much robust. Both the
326 increasing trends of heavy precipitation days and the decreasing trends of light
327 precipitation days are also obvious across China simulated by the CMIP5 models
328 (Chen and Sun, 2013; 2018), as well as the regional climate models (Gao et al., 2012).

4. Conclusions

The world is predicted to experience increased disasters, such as heat waves, flash floods, and storms, due to the continuous global warming induced by the GHG increase. The research question we aim to address in this study is how the GHG warming would affect the anthropogenic PM_{2.5} pollutions across China. Our evaluations show that the anthropogenic PM_{2.5} loadings, as well as the anthropogenic PM_{2.5} pollution days, would increase under the global warming conditions even the aerosol emissions fixed at current levels. More stringent regulations are thus suggested for regional aerosol emissions to maintain the air quality standard as the current state.

The climate changes induced by GHG warming exert their effects on the anthropogenic air pollutions across eastern China via two ways that are of interest in this study. First, the weakened tropospheric wind speed induced by the GHG warming would result in a decrease of the horizontal advection and lead to an increase in the number of stagnation days, facilitating the local accumulation of air pollutants. Second, the number of light precipitation days would decrease due to GHG-induced warming, although the total precipitation would clearly increase across China. This shift toward more no-rainfall days would further weaken the wet deposition of PM_{2.5} pollutants. Thus, the increased stagnation days and decreased light precipitation days provide a beneficial background for the occurrence of anthropogenic air pollution. Of course, under the warming scenarios, a large discrepancy exists among the different meteorological processes that benefit the air pollutions at the current state, leading to

the fuzzy recognition of air pollution change. For example, the boundary layer height shows an increase in response to the GHG warming that may strengthen the vertical dissipation of air pollutants. Thus, more studies are suggested in the future to further understand the mechanisms governing air quality across China.

Author contributions

H. P. Chen and H. J. Wang designed the research; H. P. Chen analyzed the data.

All the authors discussed the results and wrote the paper.

Competing interests

The authors declare that they have no conflict of interest.

Acknowledgements

This work is jointly supported by the National Natural Science Foundation of China (Grant No: 41421004), the National Key Research and Development Program of China (Grant No: 2016YFA0600701), and the CAS-PKU Joint Research Program.

References

- Cai, W. J., Li, K., Liao, H., Wang, H. J., and Wu, L. X.: Weather conditions conducive to Beijing severe haze more frequent under climate change, *Nature Climate Change*, 7, 257-263, 2017.
- Cao, C., Lee, X. H., Liu, S. D., Schultz, N., Xiao, W., Zhang, M., and Zhao, L.: Urban heat islands in China enhanced by haze pollution, *Nature Communications*, 7, 12509, 2016.
- Chen, H. P.: Projected change in extreme rainfall events in China by the end of the 21st century using CMIP5 models, *Chin. Sci. Bull.*, 58, 1462-1472, 2013.
- Chen, H. P., and Sun, J. Q.: Projected change in East Asian summer monsoon precipitation under RCP scenario, *Meteorol. Atmos. Phys.*, 121, 55-77, 2013.
- Chen, H. P. and Sun, J. Q.: Contribution of human influence to increased daily precipitation extremes over China, *Geophys. Res. Lett.*, 44, 2436-2444, 2017.
- Chen, H. P., and Sun, J. Q.: Projected changes in climate extremes in China in a 1.5 °C warmer world, *Int. J. Climatol.*, 38, 3607-3617, 2018.
- Chen, H. P. and Wang, H. J.: Haze days in North China and the associated atmospheric circulations based on daily visibility data from 1960 to 2012, *J. Geophys. Res. Atmos.*, 120, 5895-5909, 2015.
- Ding, Y. H. and Liu, Y. J.: Analysis of long-term variations of fog and haze in China in recent 50 years and their relations with atmospheric humidity, *Sci. China Earth Sci.*, 57, 36-46, 2014.
- Feng, J., Quan, J., Liao, H., Li, Y., and Zhao, X.: An air stagnation index to qualify

391 extreme haze events in northern China, *J. Atmos. Sci.*,
 392 doi:10.1175/JAS-D-17-0354.1, 2018.

393 Gao, H. and Li, X.: Influences of El Niño Southern Oscillation events on haze
 394 frequency in eastern China during boreal winters, *Int. J. Climatol.*, 35, 2682-2688,
 395 2015.

396 Gao, J. H., Woodward, A., Vardoulakis, S., Kovats, S., Wilkinson, P., Li, L. P., Xu, L.,
 397 Li, J., Yang, J., Li, J., Cao, L., Liu, X. B., Wu, H. X., and Liu, Q. Y.: Haze, public
 398 health and mitigation measures in China: A review of the current evidence for
 399 further policy response, *Sci. Total Environ.*, 578, 148-157, 2017.

400 Gao, X. J., Shi, Y., Zhang, D., and Giorgi, F.: Climate change in China in the 21st
 401 century as simulated by a high resolution regional climate model, *Chin. Sci. Bull.*,
 402 57, 1188-1195, 2012.

403 Han, Z. Y., Zhou, B. T., Xu, Y., Wu, J., and Shi, Y.: Projected changes in haze
 404 pollution potential in China: an ensemble of regional climate model simulations,
 405 *Atmos. Chem. Phys.*, 17, 10109-10123, 2017.

406 Horton, D. E., Harshvardhan, and Diffenbaugh, N. S.: Response of air stagnation
 407 frequency to anthropogenically enhanced radiative forcing, *Environ. Res. Lett.*, 7,
 408 044034, 2012.

409 Huang, Q., Cai, X., Song, Y., and Zhu, T.: Air stagnation in China (1985-2014):
 410 Climatological mean features and trends, *Atmos. Chem. Phys.*, 17, 7793-7805,
 411 2017.

412 Huang, Q., Cai, X., Wang, J., Song, Y., and Zhu, T.: Climatological study of the

413 boundary-layer air stagnation index for China and its relationship with air
 414 pollution, *Atmos. Chem. Phys.*, 18, 7573-7593, 2018.

415 Hurrell, J. W., Holland, M. M., Gent, P. R., Ghan, S., Kay, J. E., Kushner, P. J.,
 416 Lamarque, J. F., Large, W. G., Lawrence, D., Lindsay, K., Lipscomb, W. H.,
 417 Long, M. C., Mahowald, N., Marsh, D. R., Neale, R. B., Rasch, P., Vavrus, S.,
 418 Vertenstein, M., Bader, D., Collins, W. D., Hack, J. J., Kiehl, J., Marshall, S.: The
 419 community earth system model: A framework for collaborative research, *Bull.*
 420 *Amer. Meteorol. Soc.*, 94(9), 1339-1360, 2013.

421 Jiang, Y., Luo, Y., and Zhao, Z. C.: Projection of wind speed changes in China in the
 422 21st century by climate models (in Chinese), *Chin. J. Atmos. Sci.*, 34, 323-336,
 423 2010a.

424 Jiang, Y., Luo, Y., Zhao, Z. C., Shi, Y., Xu, Y. L., and Zhu, J. H.: Projections of wind
 425 changes for 21st century in China by three regional climate models, *Chin. Geogra.*
 426 *Sci.*, 20, 226-235, 2010b.

427 Jeong, J. I. and Park, R. J.: Winter monsoon variability and its impact on aerosol
 428 concentrations in East Asia, *Environ. Pollution*, 221, 285-292, 2017.

429 Kay, J. E., Deser, C., Phillips, A., Mai, A., Hannay, C., Strand, G., Arblaster, J. M.,
 430 Bates, S. C., Danabasoglu, G., Edwards, J., Holland, M., Kushner, P., Lamarque,
 431 J. F., Lawrence, D., Lindsay, K., Middleton, A., Munoz, E., Neale, R., Oleson, K.,
 432 Polvani, L., and Vertenstein, M.: The community earth system model (CESM)
 433 large ensemble project: A community resource for studying climate change in the
 434 presence of internal climate variability, *Bull. Amer. Meteorol. Soc.*, 96(8),

435 1333-1349, 2015.

436 Lamarque, J. F., Kyle, P. P., Meinshausen, M., Riahi, K., Smith, S. J., van Vuuren, D.
437 P., Conley, A. J., and Vitt, F.: Global and region evolution of short-lived
438 radiatively-active gases and aerosols in the Representative Concentration
439 Pathway, *Climatic Change*, 109(1), 191-212, 2011.

440 Li, H. X., Chen, H. P., Wang, H. J., and Yu, E. T.: Future precipitation changes over
441 China under 1.5 °C and 2.0 °C global warming targets by using CORDEX
442 regional climate models, *Sci. Total Environ.*, 640-641, 543-554, 2018.

443 Li, K., Liao, H., Zhu, J., and Moch, J. M.: Implications of RCP emissions on future
444 PM_{2.5} air quality and direct radiative forcing over China, *J. Geophys. Res.*
445 *Atmos.*, 121, 12985-13008, 2016.

446 Li, K., Liao, H., Cai, W. J., and Yang, Y.: Attribution of anthropogenic influence on
447 atmospheric patterns conducive to recent most severe haze over eastern China,
448 *Geophys. Res. Lett.*, 45, 2072-2081, 2018.

449 Li, Q., Zhang, R. H., and Wang, Y.: Interannual variation of the wintertime fog-haze
450 days across central and eastern China and its relation with East Asian winter
451 monsoon, *Int. J. Climatol.*, 36, 346-354, 2016.

452 Liao, H. and Chang, W. Y.: Integrated assessment of air quality and climate change for
453 policy-making-highlights of IPCC AR5 and research challenges, *National*
454 *Science Review*, 1(2), 176-179, 2014.

455 McInnes, K. L., Erwin, T. A., and Bathols, J. M.: Global climate model projected
456 changes in 10 m wind speed and direction due to anthropogenic climate change,

457 Atmos. Sci. Lett., 12, 325-333, 2011.

458 State Council: *Air pollution prevention and control action plan*. Clean Air Alliance of
 459 China Rep., 20 pp., www.cleanairchina.org/product/6349.html, 2013.

460 Stott, P. A., Stone, D. A., and Allen, M. R.: Human contribution to the European
 461 heatwave of 2003, *Nature*, 432, 610-614, 2004.

462 Tang, G. Q., Zhao, P. S., Wang, Y. H., Gao, W. K., Cheng, M. T., Xin, J. Y., Li, X., and
 463 Wang, Y. S.: Mortality and air pollution in Beijing: the long-term relationship,
 464 *Atmos. Environ.*, 150, 238-243, 2017.

465 Tie, X. X., Huang, R. J., Dai, W. T., Cao, J. J., Long, X., Su, X. L., Zhao, S. Y., Wang,
 466 Q. Y., and Li, G. H.: Effect of heavy haze and aerosol pollution on rice and wheat
 467 productions in China, *Sci. Rep.*, 6, 29612, 2016.

468 Wang, H. J.: On assessing haze attribution and control measures in China, *Atmos.*
 469 *Oceanic Sci. Lett.*, 11(2), 120-122, 2018.

470 Wang, H. J. and Chen, H. P.: Understanding the recent trend of haze pollution in
 471 eastern China: roles of climate change, *Atmos. Chem. Phys.*, 16, 4205-4211,
 472 2016.

473 Wang, H. J., Chen, H. P., and Liu, J. P.: Arctic sea ice decline intensified haze
 474 pollution in eastern China, *Atmos. Oceanic Sci. Lett.*, 8, 1-9, 2015.

475 Wang, H. J., Sun, J. Q., Chen, H. P., Zhu, Y. L., Zhang, Y., Jiang, D. B., Lang, X. M.,
 476 Fan, K., Yu, E. T., and Yang, S.: Extreme climate in China: facts, simulation and
 477 projection. *Meteorol. Z.*, 21, 279-304, 2012.

478 Wang, X., Dickinson, R., Su, L., Zhou, C., and Wang, K.: PM_{2.5} pollution in China

and how it has been exacerbated by terrain and meteorological conditions, Bull. Amer. Meteorol. Soc., 99(1), 105-119, 2018.

World Health Organization: *Air quality guidelines: Global update 2005*. World Health Organization Rep., 496 pp., www.euro.who.int/_data/assets/pdf_file/0005/78638/E90038.pdf/, 2014.

Xiao, D., Li, Y., Fan, S. J., Zhang, R. H., Sun, J. R., and Wang, Y.: Plausible influence of Atlantic Ocean SST anomalies on winter haze in China, Theor. Appl. Climatol., 122, 249-257, 2015.

Xu, Y. Y., and Lin, L.: Pattern scaling based projections for precipitation and potential evapotranspiration: sensitivity to composition of GHGs and aerosols forcing, Climatic Change, 140, 635-647, 2017.

Xu, Y. Y. and Lamarque, J. F.: Isolating the meteorological impact of 21st century GHG warming on the removal and atmospheric loading of anthropogenic fine particulate matter pollution at global scale, Earth's Future, 6, 428-440, 2018.

Yang, Y., Liao, H., and Lou, S. J.: Increase in winter haze over eastern China in recent decades: roles of variations in meteorological parameters and anthropogenic emissions, J. Geophys. Res. Atmos., 121, 13050-13065, 2016.

Yang, Y., Russell, L. M., Lou, S. J., Liao, H., Guo, J. P., Liu, Y., Singh, B., and Ghan, S. J.: Dust-wind interactions can intensify aerosol pollution over eastern China, Nature communications, 8, 15333, 2017a.

Yang, Y., Wang, H. L., Smith, S. J., Ma, P. L., and Rasch, P. J.: Source attribution of black carbon and its direct radiative forcing in China, Atmos. Chem. Phys., 17,

4319-4336, 2017b.

Yang, Y., Wang, H. L., Smith, S. J., Easter, R., Ma, P. L., Qian, Y., Yu, H. B., Li, C.,
and Rasch, P. J.: Global source attribution of sulfate concentration and direct and
indirect radiative forcing, *Atmos. Chem. Phys.*, 17, 8903-8922, 2017c.

Yin, Z. C. and Wang, H. J.: The relationship between the subtropical Western Pacific
SST and haze over North-Central North China Plain, *Int. J. Climatol.*, 36,
3479-3491, 2016.

Yin, Z. C., Wang, H. J., and Chen, H. P.: Understanding severe winter haze events in
the North China Plain in 2014: roles of climate anomalies, *Atmos. Chem. Phys.*,
17, 1641-1651, 2017.

Yin, Z. C., Wang, H. J., and Yuan, D. M.: Interdecadal increase of haze in winter over
North China and the Huang-huai area and the weakening of the East Asia winter
monsoon (in Chinese), *Chin. Sci. Bull.*, 60, 1395-1400, 2015.

Zhang, R. H., Li, Q., and Zhang, R. N.: Meteorological conditions for the persistent
severe fog and haze event over eastern China in January 2013, *Sci. China Earth
Sci.*, 57, 26-35, 2014.

Zhang, Y., Ding, A. J., Mao, H. T., Nie, W., Zhou, D. R., Liu, L. X., Huang, X., and Fu,
C. B.: Impact of synoptic weather patterns and inter-decadal climate variability
on air quality in the North China plain during 1980-2013, *Atmos. Environ.*, 124,
119-128, 2016a.

Zhang, Z., Zhang, X., Goog, D., Kim, S., Mao, R., and Zhao, X.: Possible influence of
atmospheric circulations over winter haze pollution in the Beijing-Tian-Hebei

523 region, northern China, Atmos. Chem. Phys., 16, 561-571, 2016b.

524 Zhao, S., Li, J. P., and Sun, C.: Decadal variability in the occurrence of wintertime

525 haze in central eastern China tied to the Pacific Decadal Oscillation, Sci. Rep., 6,

526 27424, 2016.

527 Zhao, S. Y., Zhang, H., and Xie, B.: The effects of El Niño-Southern Oscillation on

528 the winter haze pollution of China, Atmos. Chem. Phys., 18, 1863-1877, 2018.

529

Figure captions

Figure 1. Observed PM_{2.5} pollution conditions over eastern China during the past years. (a) Annual averaged PM_{2.5} concentration ($\mu\text{g}/\text{m}^3$) for the years of 2015-2017. (b) Variations of annual averaged PM_{2.5} concentration (green bars) in Beijing city and the corresponding number of the severe PM_{2.5} pollution days (red bars). The severe pollution days are defined as the daily averaged PM_{2.5} concentration exceeding 75 $\mu\text{g}/\text{m}^3$. (c), (d), and (e) are similar to (b), but for the results of Shanghai, Guangzhou, and Chengdu city, respectively.

Figure 2. Plots of future changes of the total PM_{2.5} as well as its associated species averaged over eastern China in terms of the surface concentration ($\mu\text{g}/\text{m}^3$, right axis in red) and column burden (mg/m^2 , left axis in blue) from the simulations of the RCP8.5_FixAerosol2005 experiment. (a) PM_{2.5}, (b) BC, (c) SO₄, (d) POM, and (e) SOA. Ensemble variance (1 sigma) for surface concentration is shown in red shadings.

Figure 3. Changes of the anthropogenic PM_{2.5} pollution days across eastern China from the RCP8.5_FixAerosol2005 experiment. The top panel (a, b) shows the changes of light air pollution days ($> 25 \mu\text{g}/\text{m}^3$) and the bottom panel (c, d) shows the results of severe air pollution days ($> 75 \mu\text{g}/\text{m}^3$). The left panel (a, c) illustrates the annual averaged severe pollution days in 2006-2015 and the right panel (b, d) shows changes of the pollution days at the end of the 21st century with respect to 2006-2015. Dots in (b) and (d) mean the changes are significant at the 95% confidence level using Student T-test for all years and ensembles. Units: days.

Figure 4. Attributable changes of anthropogenic air pollution days to the increased greenhouse gases emissions. (a) Spatial distribution of FAR for the changes of severe PM_{2.5} pollutions ($> 75 \mu\text{g}/\text{m}^3$) at the end of the 21st century over eastern China. (b) Regional averaged relative changes of air pollution days (left axis in red; $> 25 \mu\text{g}/\text{m}^3$) and the corresponding variation of FAR (right axis in blue). Ensemble variance (1 sigma) for the relative changes of pollution days is shown in red shadings. (c) is similar to (b), but for the severe PM_{2.5} pollution days. Units: %.

Figure 5. Simulated changes in weather conditions of the air pollutions across eastern China due to the GHG-induced warming. (a) Changes of the planetary boundary layer height (PBLH) at the end of the 21st century with respect to the years of 2006-2015 from the RCP8.5_FixAerosol2005 experiment. (b) and (c) are similar to (a) but for the wind speed at near-surface and 500-hPa levels, respectively. (d) Changes in the light precipitation days (daily accumulated precipitation $< 10 \text{ mm}$) at the end of the 21st century with respect to the current state. (e) is similar to (d) but for the heavy precipitation days ($> 10 \text{ mm}$). Dots in the figure mean the changes are significant at the 95% confidence level using Student T-test for all years and ensembles. Units: %.

Figure 6. Changes in the stagnant conditions across China due to the GHG-induced warming. (a) Distribution of the relative changes of the stagnation days at the end of the 21st century against the current state (2006-2015). Dots mean the changes are significant at the 95% confidence level using Student T-test for all years and ensembles. (b) Variations of the regional averaged stagnation days over

574 eastern China. Ensemble variance (1 sigma) is shown in red shadings. (c), (d), (e), and
575 (f) are similar to (b), but for the results of four Chinese economic zones, i.e., JJJ, YRD,
576 PRD, and SCB. Units: %.

577

578

Figures

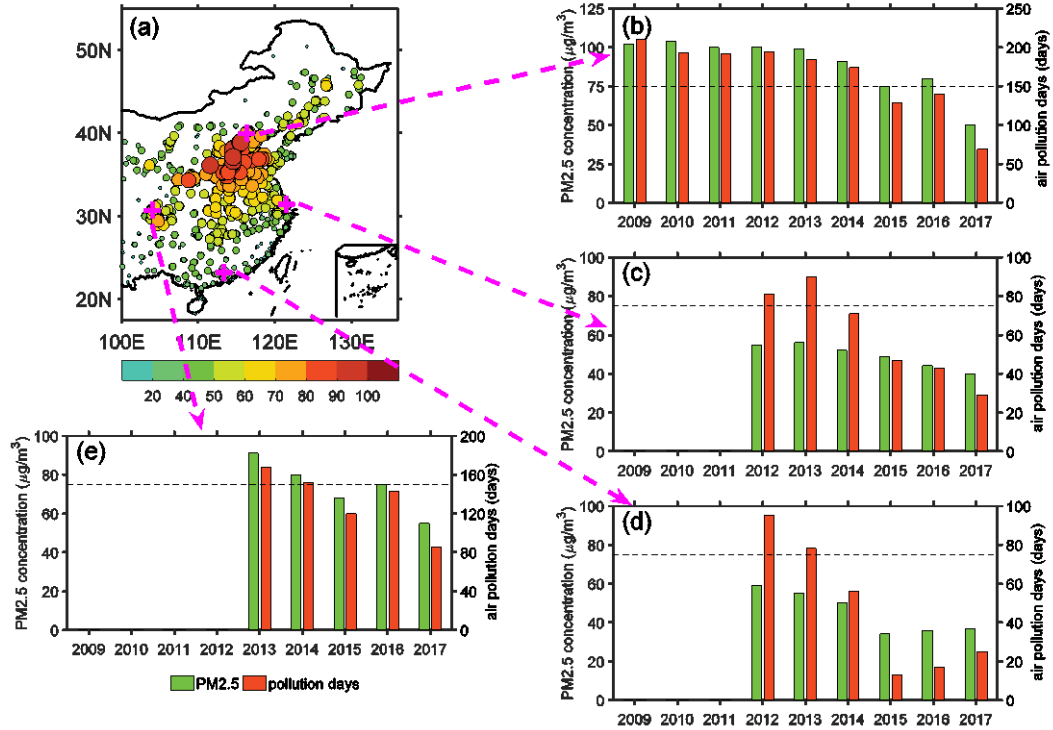


Figure 1. Observed PM_{2.5} pollution conditions over eastern China during the past years. (a) Annual averaged PM_{2.5} concentration (μg/m³) for the years of 2015-2017. (b) Variations of annual averaged PM_{2.5} concentration (green bars) in Beijing city and the corresponding number of the severe PM_{2.5} pollution days (red bars). The severe pollution days are defined as the daily averaged PM_{2.5} concentration exceeding 75 μg/m³. (c), (d), and (e) are similar to (b), but for the results of Shanghai, Guangzhou, and Chengdu city, respectively.

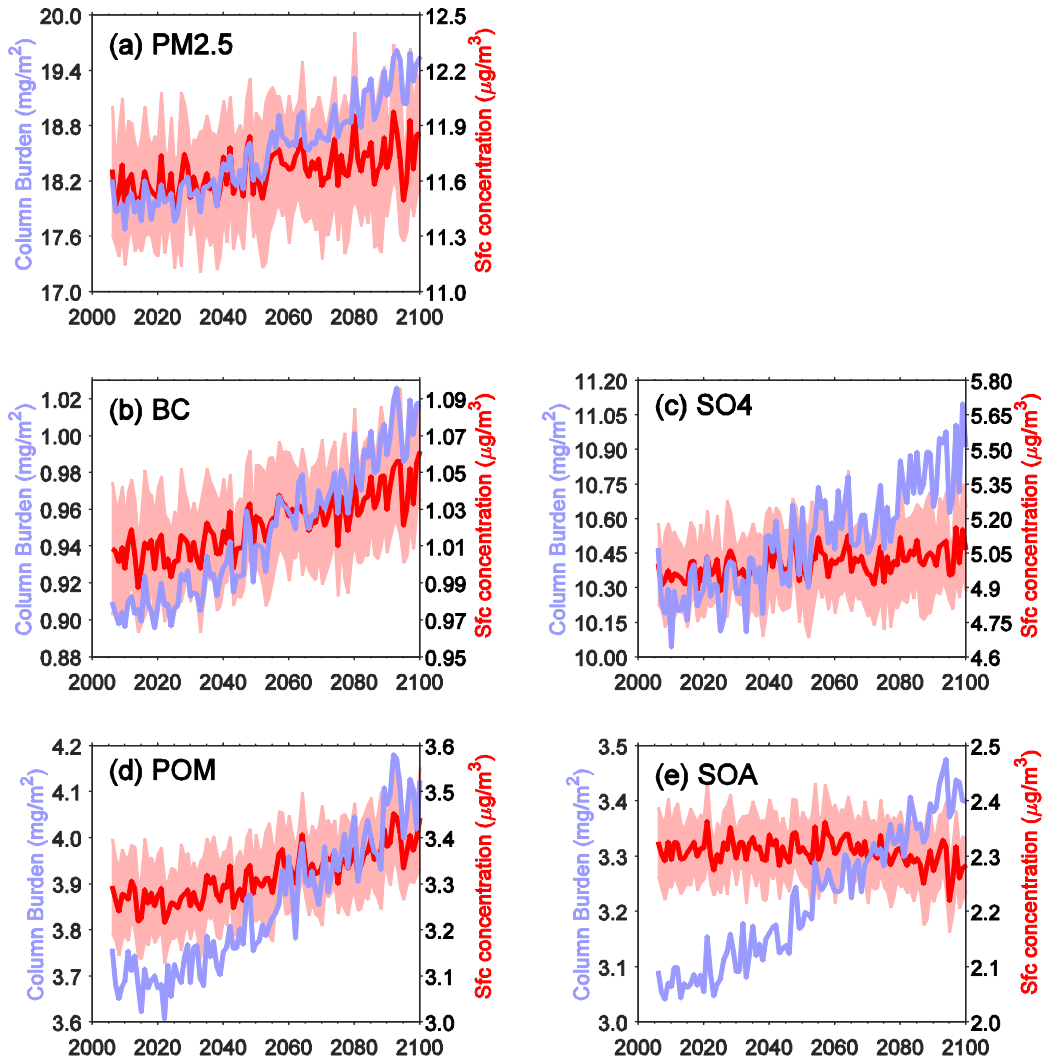


Figure 2. Plots of future changes of the total PM_{2.5} as well as its associated species averaged over eastern China in terms of the surface concentration ($\mu\text{g}/\text{m}^3$, right axis in red) and column burden (mg/m^2 , left axis in blue) from the simulations of the RCP8.5_FixAerosol2005 experiment. (a) PM_{2.5}, (b) BC, (c) SO₄, (d) POM, and (e) SOA. Ensemble variance (1 sigma) for surface concentration is shown in red shadings.

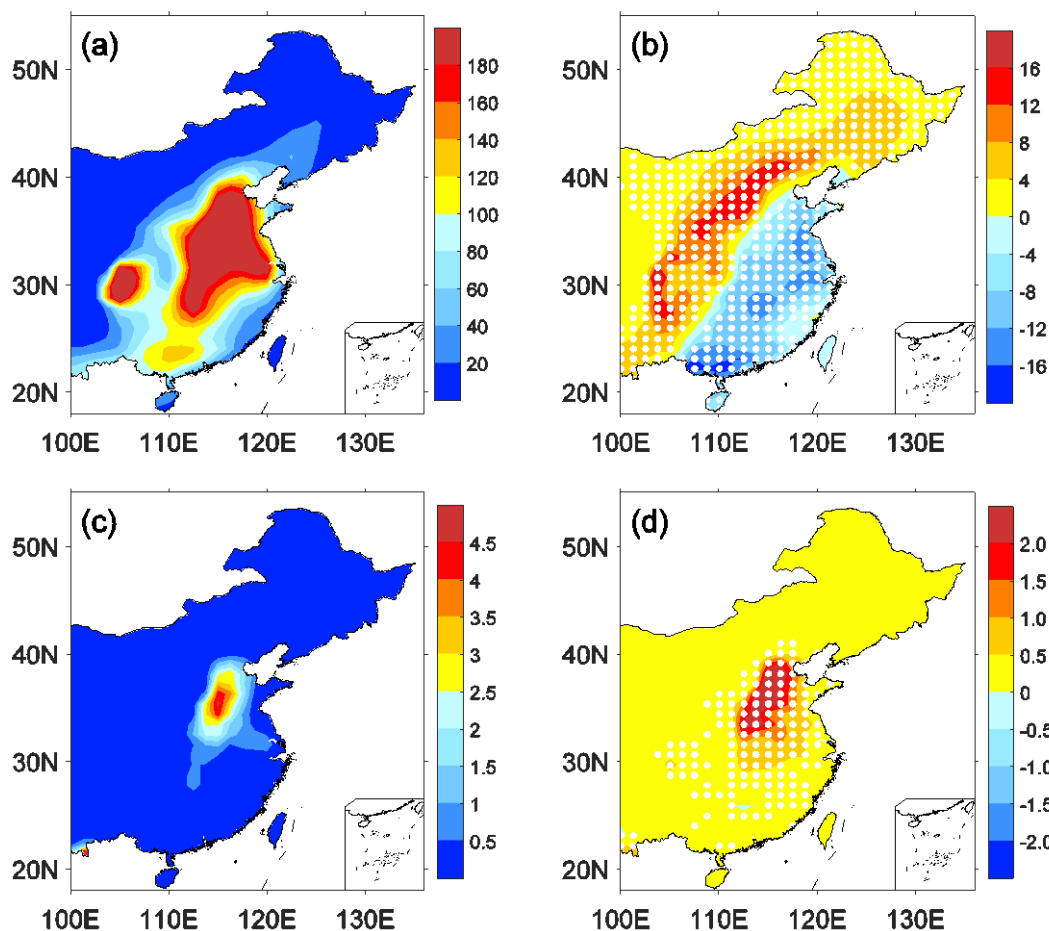


Figure 3. Changes of the anthropogenic PM_{2.5} pollution days across eastern China from the RCP8.5_FixAerosol2005 experiment. The top panel (a, b) shows the changes of light air pollution days ($> 25 \mu\text{g}/\text{m}^3$) and the bottom panel (c, d) shows the results of severe air pollution days ($> 75 \mu\text{g}/\text{m}^3$). The left panel (a, c) illustrates the annual averaged severe pollution days in 2006-2015 and the right panel (b, d) shows changes of the pollution days at the end of the 21st century with respect to 2006-2015. Dots in (b) and (d) mean the changes are significant at the 95% confidence level using Student T-test for all years and ensembles. Units: days.

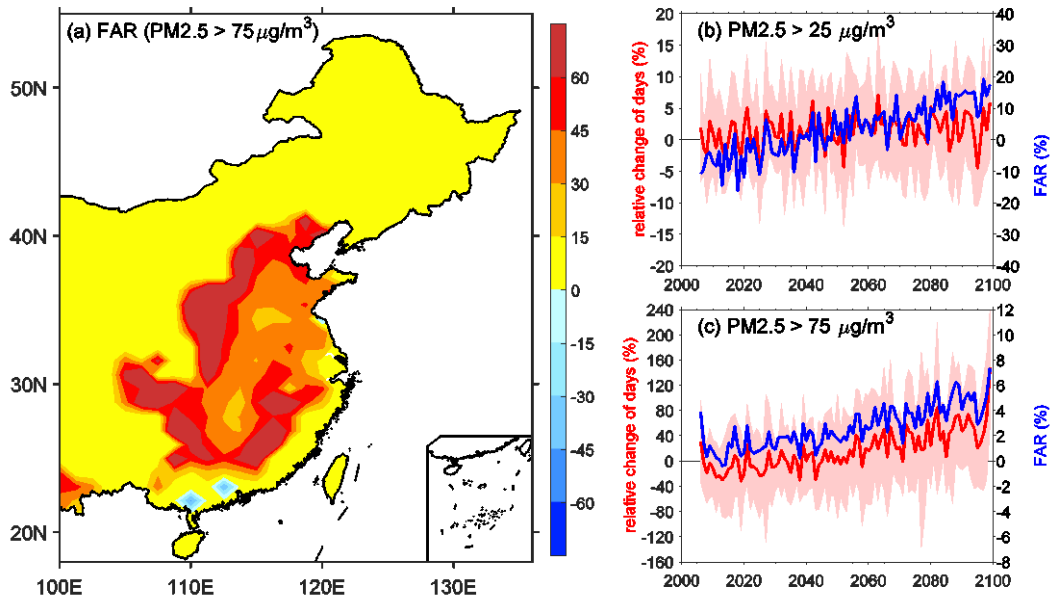


Figure 4. Attributable changes of anthropogenic air pollution days to the increased greenhouse gases emissions. (a) Spatial distribution of FAR for the changes of severe PM_{2.5} pollutions (> 75 µg/m³) at the end of the 21st century over eastern China. (b) Regional averaged relative changes of air pollution days (left axis in red; > 25 µg/m³) and the corresponding variation of FAR (right axis in blue). Ensemble variance (1 sigma) for the relative changes of pollution days is shown in red shadings. (c) is similar to (b), but for the severe PM_{2.5} pollution days. Units: %.

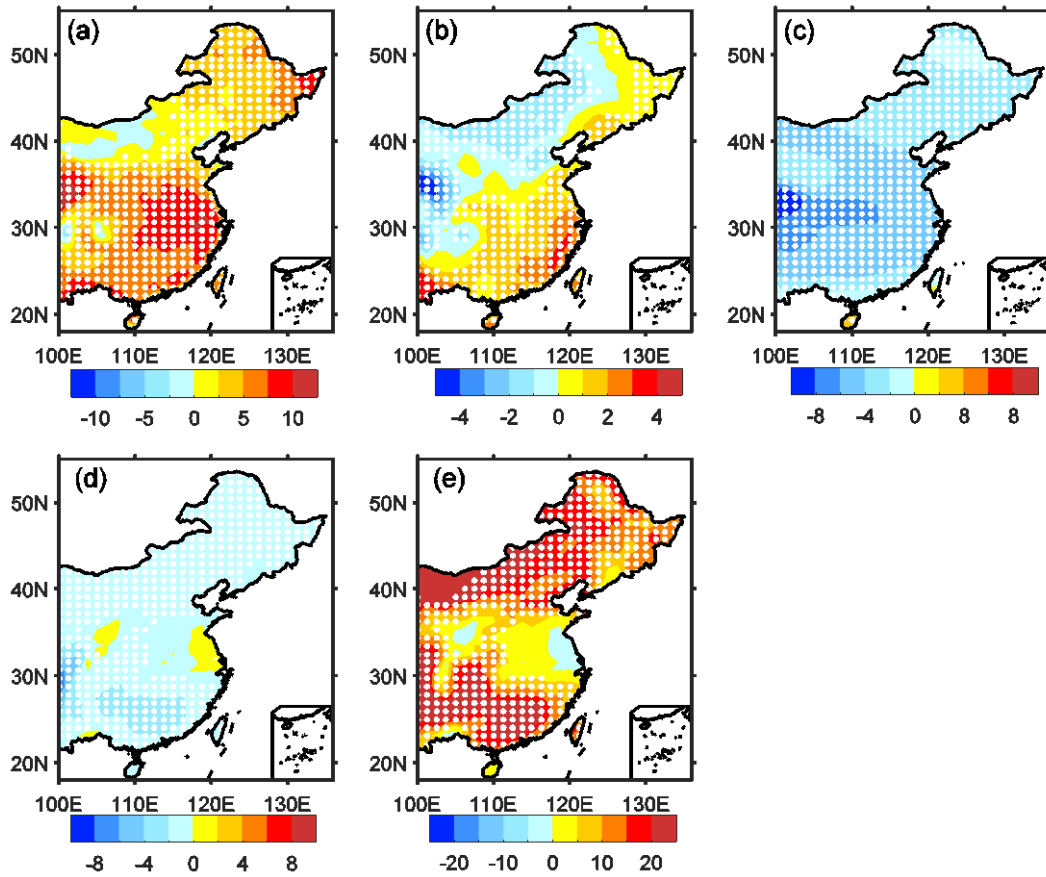


Figure 5. Simulated changes in weather conditions of the air pollutions across eastern China due to the GHG-induced warming. (a) Changes of the planetary boundary layer height (PBLH) at the end of the 21st century with respect to the years of 2006-2015 from the RCP8.5_FixAerosol2005 experiment. (b) and (c) are similar to (a) but for the wind speed at near-surface and 500-hPa levels, respectively. (d) Changes in the light precipitation days (daily accumulated precipitation < 10 mm) at the end of the 21st century with respect to the current state. (e) is similar to (d) but for the heavy precipitation days (> 10 mm). Dots in the figure mean the changes are significant at the 95% confidence level using Student T-test for all years and ensembles. Units: %.

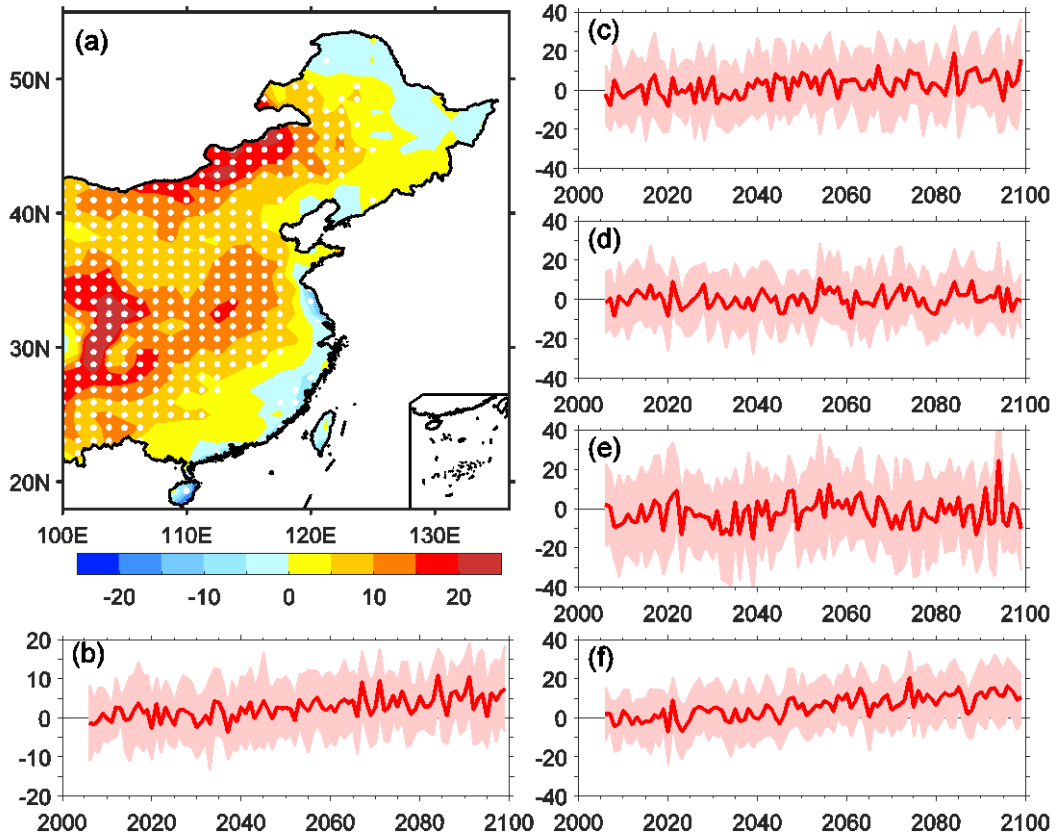


Figure 6. Changes in the stagnant conditions across China due to the GHG-induced warming. (a) Distribution of the relative changes of the stagnation days at the end of the 21st century against the current state (2006-2015). Dots mean the changes are significant at the 95% confidence level using Student T-test for all years and ensembles. (b) Variations of the regional averaged stagnation days over eastern China. Ensemble variance (1 sigma) is shown in red shadings. (c), (d), (e), and (f) are similar to (b), but for the results of four Chinese economic zones, i.e., JJJ, YRD, PRD, and SCB. Units: %.